PRIMER

DNA origami

Swarup Dey[1], Chunhai Fan[2,3]✉, Kurt V. Gothelf[4,5]✉, Jiang Li[2,6]✉, Chenxiang Lin[7,8]✉, Longfei Liu[7,8], Na Liu[9,10]✉, Minke A. D. Nijenhuis[4,5], Barbara Saccà[11]✉, Friedrich C. Simmel[12]✉, Hao Yan[1]✉ and Pengfei Zhan[9,10]

Abstract | Biological materials are self-assembled with near-atomic precision in living cells, whereas synthetic 3D structures generally lack such precision and controllability. Recently, DNA nanotechnology, especially DNA origami technology, has been useful in the bottom-up fabrication of well-defined nanostructures ranging from tens of nanometres to sub-micrometres. In this Primer, we summarize the methodologies of DNA origami technology, including origami design, synthesis, functionalization and characterization. We highlight applications of origami structures in nanofabrication, nanophotonics and nanoelectronics, catalysis, computation, molecular machines, bioimaging, drug delivery and biophysics. We identify challenges for the field, including size limits, stability issues and the scale of production, and discuss their possible solutions. We further provide an outlook on next-generation DNA origami techniques that will allow in vivo synthesis and multiscale manufacturing.

Holliday junction
A four-stranded cross-shaped DNA structure (named after British geneticist Robin Holliday) that forms during the process of genetic recombination.

DNA nanotechnology
A branch of nanotechnology concerned with the design, study and application of DNA-based synthetic structures to take advantage of the physical and chemical properties of DNA.

DNA tiles
DNA structures that as building blocks can be tiled into higher order (usually periodic) structures.

✉*e-mail: fanchunhai@sjtu.edu.cn; kvg@chem.au.dk; lijiang@zjlab.org.cn; chenxiang.lin@yale.edu; na.liu@pi2.uni-stuttgart.de; barbara.sacca@uni-due.de; simmel@tum.de; hao.yan@asu.edu*

https://doi.org/10.1038/s43586-020-00009-8

Biological materials of living cells are synthesized in a bottom-up manner. The information encoded in biomolecules is exploited to guide their own self-assembly and the hierarchical formation of larger complexes, keeping near-atomic precision along sizes spanning from nanometres to the macroscopic scale. By contrast, in vitro manufacturing of complex 3D structures down to the nanometre scale has usually lacked such precision and controllability. In the 1980s, Seeman first proposed the rational design of an immobile Holliday junction[1], which turned DNA into a nanoscale polymer extending in two dimensions instead of simple 1D double helices. This work signalled the debut of DNA nanotechnology, which allows massively parallel synthesis of well-defined nanostructures, with synthesis on a picomole-scale generating 10^{12} copies of a product. Since then, various DNA nanostructures including double-crossover[2], triple-crossover[3], 4 × 4 (REF.[4]) and three-point star structures[5] have been assembled using the junction of multiple short single-stranded DNAs (ssDNAs). These DNA tiles can be further assembled into periodic superstructures including nanotubes, 2D lattices and 3D structures including polyhedra, hydrogels and crystals[6].

DNA origami technology, as a promising branch of DNA nanotechnology, is an effective technique for bottom-up fabrication of well-defined nanostructures ranging from tens of nanometres to sub-micrometres. DNA origami involves the folding of DNA to create 2D and 3D objects at the nanoscale. The concept of DNA origami relies on folding a long ssDNA called the scaffold (typically viral DNA ~7,000 nucleotides long), with hundreds of designed short ssDNAs called staples. Each staple has multiple binding domains that bind and bring together otherwise distant regions of the scaffold via crossover base pairing, folding the scaffold in a manner analogous to knitting[7] (FIG. 1A). The geometries of the resulting structures can be programmed with the staple sequences. This programmability enables computer-aided design and universal synthesis protocols[8–10] that make DNA origami an easy to use technology amenable to automated fabrication. Compared with tile-based DNA assembly strategies, DNA origami synthesis generally exhibits higher yield, robustness and the ability to build complex non-periodic shapes, which partially arises from the high cooperativity of multiple scaffold–staple interactions during origami folding[11,12]. Since the original demonstration of 2D patterns[7] (FIG. 1B), virtually any arbitrary shape can be synthesized, from 1D to 3D structures with user-defined asymmetry[13–15], cavities[16,17] or curvatures[18,19] (FIG. 1C). More recent progress includes hierarchical assembly of supramolecular structures[20–22] (FIG. 1D), single-stranded origami[23,24] (FIG. 1E) and dynamic structures[6,25,26] (BOX 1; FIG. 1F).

A typical planar DNA origami structure contains approximately 200 staples with unique sequences and positions, which can serve as uniquely addressable points in an area of 8,000–10,000 nm^2 (REF.[6]). The global addressability with nanometre resolution allows the structures to serve as elaborate pegboards or frameworks; by prescribing functional moieties on staples, various types of material can be site-specifically placed at specified locations on a DNA origami structure[6,27]. These achievements have shown great promise in the fabrication of structures enhanced by metal, silica, lipid

Author addresses

[1]Center for Molecular Design and Biomimetics, The Biodesign Institute, School of Molecular Sciences, Arizona State University, Tempe, AZ, USA.
[2]School of Chemistry and Chemical Engineering, Frontiers Science Center for Transformative Molecules, National Center for Translational Medicine, Shanghai Jiao Tong University, Shanghai, China.
[3]Institute of Molecular Medicine, Shanghai Key Laboratory for Nucleic Acids Chemistry and Nanomedicine, Renji Hospital, School of Medicine, Shanghai Jiao Tong University, Shanghai, China.
[4]Interdisciplinary Nanoscience Center (iNANO), Aarhus University, Aarhus, Denmark.
[5]Department of Chemistry, Aarhus University, Aarhus, Denmark.
[6]Bioimaging Center, Shanghai Synchrotron Radiation Facility, Zhangjiang Laboratory, Shanghai Advanced Research Institute, Chinese Academy of Sciences, Shanghai, China.
[7]Department of Cell Biology, Yale University School of Medicine, New Haven, CT, USA.
[8]Nanobiology Institute, Yale University, West Haven, CT, USA.
[9]2nd Physics Institute, University of Stuttgart, Stuttgart, Germany.
[10]Max Planck Institute for Solid State Research, Stuttgart, Germany.
[11]Centre for Medical Biotechnology (ZMB), University of Duisburg–Essen, Essen, Germany.
[12]Physics Department, Technische Universität München, Garching, Germany.

or polymer coatings[28–30] and as nanosystems for nanophotonic and nanoelectronic devices[31–36]. Dynamic DNA origami structures can be rationally engineered on the basis of structurally reconfigurable modules (FIG. 1f) that use strand displacement reactions[25,37], conformationally switchable domains and base stacking components[26], enabling various applications such as target-responsive biosensing and bioimaging[38], smart drug delivery[39,40], biomolecular computing[41] and nanodevices allowing external manipulation with light or other electromagnetic fields[42–44].

In this Primer, we summarize the methodologies of DNA origami technology, including origami design, synthesis, functionalization and characterization (Experimentation and Results). We highlight applications of origami structures in nanofabrication, nanophotonics/nanoelectronics, catalysis, computation, molecular machines, bioimaging, drug delivery and biophysics (Applications). We provide caution for using DNA origami with high reproducibility and reliability (Reproducibility and data deposition). We identify challenges for the field, including size limits, stability issues and the scale of production, and discuss their possible solutions (Limitations and optimizations). Finally, we discuss next-generation DNA origami techniques that will allow in vivo synthesis and manufacturing of multiscale-ordered materials (Outlook).

Experimentation

DNA origami objects with a rich diversity in dimension, geometry and shape have been produced, ranging from single layers to multilayers[7,17] as well as from flexible wireframes to rigid polyhedra[15,19,45]. A typical experimental process for fabricating DNA origami is illustrated in FIG. 2.

Design. The basic principle of DNA origami design is to translate the desired final shape into the folding route of a given scaffold and generate corresponding staple sequences that can fulfil the folding. TABLE 1 presents a comparative summary of the different software developed for designing DNA origami structures.

The first-generation (1G) DNA origami design tools (for example, caDNAno[8]) were developed for designing various 2D and 3D origami structures. Detailed insights into designing origami by 1G software have been covered extensively elsewhere[46] and can also be found in the references cited in TABLE 1. caDNAno remains the most mature and routinely used software for designing DNA origami[8] (FIG. 2a). Other software such as Tiamat, SARSE-DNA, Nanoengineer-1, Hex-tiles, GIDEON, K-router and so on have also been used for DNA origami designs. These 1G design software require manual scaffold routing, and manual — or semi-automated, in the case of caDNAno — scaffold and staple crossover creation, requiring extensive expertise on this structure type and more technical knowledge for design of DNA origami.

Second-generation (2G) design software have been developed to be more user-friendly and demand less technical knowledge than their 1G counterparts. The main advantage of using 2G software is the ability to generate staple sequences in an automated fashion from user-provided 3D designs. vHelix[15] is the most widely used software in this category and also contains an integrated simulation platform that can predict the folding of the designed structures in standard DNA origami folding buffers. Other software such as DAEDALUS[47] and TALOS[9] for 3D origami and vHelix-BSCOR[48], PERDIX[49] and METIS[10] for 2D origami are also available. Other automated design tools such as MagicDNA[50] have been reported in preprints.

Recently, two new software have been reported that enhance the capabilities of DNA origami design by combining features from the 1G and 2G software. ATHENA[51] integrates features of other existing 2G software, specifically that of DAEDALUS, PERDIX, TALOS and METIS. Adenita[52] is an open source platform that combines almost all of the 1G and 2G design software capabilities. It can design lattice-based wireframes, multilayered structures, free-form tiles and single-stranded tiles. Adenita also contains an integrated simulation platform to predict the stability of the designed structures in buffer after their formation. ATHENA and, especially, Adenita are currently the most versatile design software available and they offer unprecedented user-friendly interfaces. Being integrated with the commercial nanoscale simulation software SAMSON, Adenita is the only software that also accommodates other biomolecules such as protein, lipid or drug molecules. This is expected to improve origami manufacturing feasibility as well as versatility of design for experts and non-experts alike. We therefore label Adenita and ATHENA as third-generation (3G) design software. One considerable drawback of 2G and 3G software is that they are more recent and less widely tested across different laboratories. FIGURE 2 presents a decision-making flowchart to choose the right design software for designing DNA origami.

Screening many different origami designs thoroughly through experimental work can be challenging. It is therefore important to predict the folding of designed origami computationally. All-atom molecular dynamics simulation has been successfully used

DNA origami
A class of technologies for building DNA nanostructures by folding a long single-stranded DNA (scaffold) into desired shapes via base pairing.

Scaffold
A long single-stranded DNA serving as the major component of a DNA origami structure, which will be folded into a defined shape.

Staples
Short single-stranded DNAs that help fold the scaffold DNA via crossover base pairing.

Addressable points
The locations of staple DNAs, including their extensions or modifications, on a DNA origami structure. These points can be prescribed as each staple has a globally unique base sequence (a unique address).

Base stacking
A stacking arrangement of the planes of nucleobases or base pairs in the structure of nucleic acids, leading to a strong π–π interaction vertical to the planes, which is a major force that stabilizes DNA duplex structures.

for characterizing the structural, mechanical and ionic conductive properties of DNA origami in microscopic detail at the DNA single base pair level[53,54]. However, owing to the substantial sizes of DNA origami structures and the microsecond to millisecond timescales of complex events such as hybridization and dehybridization, it is computationally too expensive to use conventional all-atom molecular dynamics simulation packages such as AMBER[55], NAMD[56,57] and GROMACS[58] for DNA origami structure predictions. Web server-based coarse-graining packages such as CanDo[56] and COSM[59] offer prediction of mechanical strain in designed origami structures that help minimize undesired folding in the assembly. A more comprehensive web server-based package, oxDNA[60–62] offers the most versatile and practical approach in terms of ease of usage and features. oxDNA.org is as an entirely web-based application that uses rigid-body simulation to predict more advanced structural features such as the root mean square fluctuation structure, average hydrogen-bond occupancy, distance between user-specified nucleotides and angle between each duplex in the nanostructure. oxView, the graphical user interface of oxDNA, also offers de novo design of DNA nanostructures that is particularly useful when manipulating previously published designs for specific applications based on oxDNA simulations. The recently reported MrDNA[63], which can perform all-atom molecular dynamics simulation within 30 min, offers the highest resolution as well as the fastest speed compared with other simulation packages such as oxDNA. The bottleneck for using MrDNA, however, is the requirement for parallel computing such as a CUDA-enabled graphical processing unit in a supercomputing cluster to run simulations, which is resource-intensive and needs significant coding knowledge. The choice of appropriate simulation packages is often determined based on the target applications and availability of resources[60–63].

Assembly. The choice of the scaffold to use for DNA origami is determined by the size and complexity of the desired structure. The most commonly used scaffold

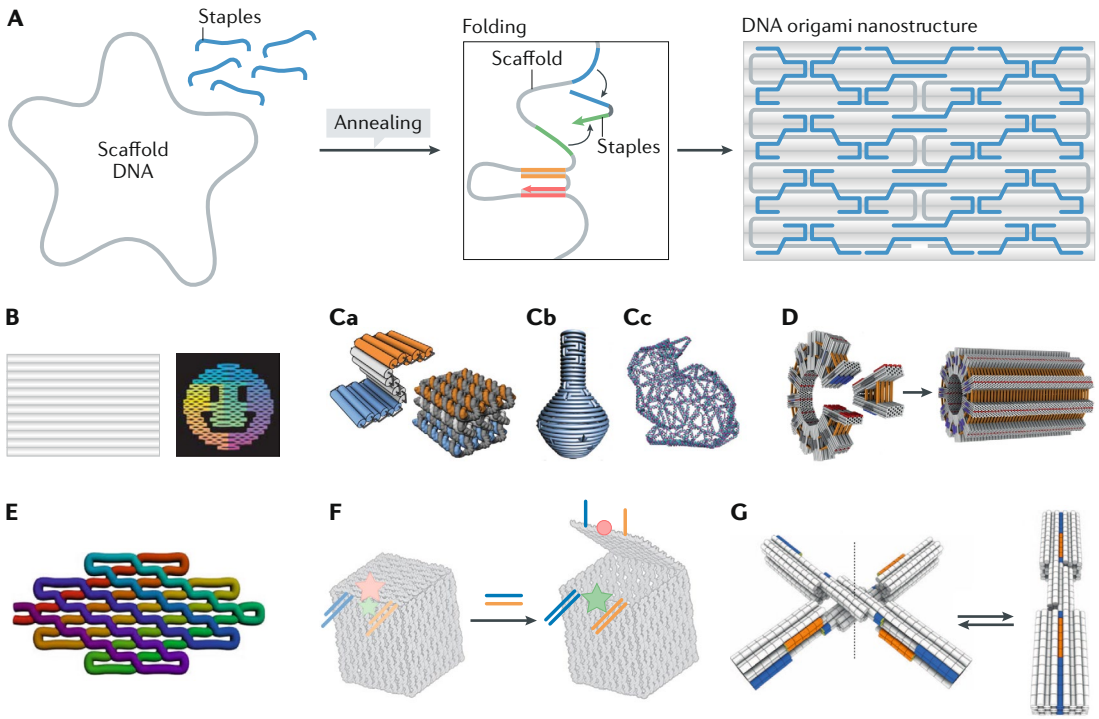

Fig. 1 | **DNA origami technology. A** | Principle of classic DNA origami. A long single-stranded scaffold DNA is annealed with multiple short staples (blue). The staples can bring together distant regions of the scaffold via base pairing (pairing sequences are marked red, orange, green and blue, for example), resulting in a prescribed shape. **B** | Representative 2D planar DNA origami shapes[7]. **C** | 3D nanostructures depicting a honeycomb lattice[17] (part **Ca**), a structure with complex curvature[19] (part **Cb**) and a wireframe structure with arbitrary shape[15] (part **Cc**). **D** | Superstructures hierarchically assembled from multiple DNA origami structures[20]. **E** | Single-stranded DNA/RNA origami[23]. The rainbow gradient represents the folding route starting from the 5′ and 3′ ends (red) to the middle of the strand (purple). **F**,**G** | Examples of dynamic DNA origami nanostructures: a DNA origami box[89] whose lid is initially locked by two DNA duplexes and can be opened via strand displacement by oligonucleotide keys (blue and orange lines, lock and key strands; pink and green stars, fluorescent emission from Cy5 and Cy3 labelling; red circle, Cy5 lost emission) (part **F**); and a dynamic nanodevice[26] switchable between two conformations (open and closed) upon the competition between base stacking (arising from the complement of blue and orange domains) and electrostatic repulsion, which is responsive to the change in temperature and/or Mg^{2+} concentration (part **G**). Part **B** adapted from REF.[7], Springer Nature Limited. Part **Ca** adapted from REF.[17], Springer Nature Limited. Part **Cb** adapted with permission from REF.[19], AAAS. Part **Cc** adapted from REF.[15], Springer Nature Limited. Part **D** adapted from REF.[20], Springer Nature Limited. Part **E** adapted from REF.[23], AAAS. Part **F** adapted from REF.[89], Springer Nature Limited. Part **G** adapted with permission from REF.[26], AAAS.

Box 1 | **Timeline of representative advances in the field of DNA origami**

2006
- The invention of DNA origami[7]

2009
- 3D DNA origami with twists and curvatures[17,18]
- Configurable DNA box[89]
- Placement of DNA origami on lithographic patterns[140]
- Alignment of carbon nanotubes with DNA origami[32]
- Single-molecule super-resolution imaging[219]

2010
- Walkers on DNA origami[179]
- Single-molecule reactions on DNA origami[305]

2011
- 2D crystalline arrays[77]
- 3D structures with complex curvatures[19]

2012
- Chiral plasmonic nanostructures[118]
- Synthetic lipid membrane channels[306]
- Responsive logic-gated nanorobot for smart delivery[184]

2014
- RNA origami[24]
- DNA moulds[16]

2015
- Non-canonical assembly via shape complement[26]
- 3D modelling with polyhedral meshes[15]
- Routing conjugated polymers[307]

2016
- Top-down automatic design[47]
- Precise placement of DNA origami for hybrid nanodevice[139]
- Diamond family of nanoparticle superlattices[125]
- DNA-templated liposomes[253]
- Forcemeters[225,240]

2017
- Protein–DNA origami[303]
- Large single-stranded DNA and RNA origami[23]
- Supersized structures formed by DNA origami[20,21]
- Mass production of DNA origami[285]
- Plasmonic waveguide[144]
- Cargo-sorting DNA robot[42]

2018
- Biomineralization of DNA origami[28]
- 3D DNA origami crystals[82]
- The concept of framework nucleic acids[27]
- Electric field-driven nanoscale robotic arms[110]
- Intelligent cancer therapy and renal therapy[40,195]

2019
- Enzyme-driven DNA origami rotors[223]
- Single-molecule DNA navigator[43]
- Free-style metallization[131,308]

2020
- Single-molecule analysis of biomolecular interactions[215,248,309,310]

is the m13mp18 viral genome 7,249 nucleotides long isolated from the M13 phage. Other typical scaffolds include p7308, p7560 and p8064, also derived from M13, which provide alternative scaffold lengths and sequences. These scaffolds can be purchased from companies, such as New England Biolabs, Guild Biosciences, Tilibit Nanosystems, Integrated DNA Technologies (IDT) and so on, or custom-made using asymmetrical PCR[64], using enzymatic single-strand digestion of PCR-amplified double-stranded DNA (dsDNA)[65] or by purifying phage-derived single-stranded genomic DNA[66,67]. Custom scaffold sequences can provide better control of the overall size of the final object. However, scaffolds derived from phages require inclusion of multi-kilobase DNA sequences that cannot be altered or removed, constraining design possibilities. Breaking away from the M13 genome in terms of production of scaffolds with custom size (short and long) and sequence could provide more design possibilities and enhance development of the DNA origami method[68]. Clearly, the size of a single DNA origami structure is limited by the length of the scaffold used for folding. Efforts in scaling up the dimensions of origami units include the use of longer single-stranded scaffolds[64,65,67] or the application of short scaffold-parity strands[69]. This strategy uses a set of randomly generated sequences typically 42 nucleotides long that are complementary to segments of staples extending from the origami shape and partially hybridized to the scaffold. In this way, additional helical layers can be bound to the scaffold-related origami structure, eventually enlarging its dimensions. After exporting the sequences of the designed staples from the software as .csv or .txt files, the staple strands are mainly purchased in the form of synthesized oligonucleotides in 96-well plates (from, for example, IDT or ThermoFisher Scientific).

Given that the stability of DNA base pairing is sensitive to cation concentration, the yield of DNA origami structures in terms of the fraction of correct structures is highly dependent on cation concentration. Most protocols for the assembly of DNA origami involve pH 8 Tris–acetate–EDTA (TAE) buffers with different concentrations (5–20 mM) of Mg^{2+} ($MgCl_2$). The optimal concentration of Mg^{2+} varies with the complexity of the DNA origami structures. The most commonly used buffer contains 12.5 mM Mg^{2+}. Higher concentrations (16.5–20 mM) are used for 3D structures, where higher base pairing stability is desired to maintain highly folded conformations, whereas lower concentrations (5–10 mM) are used for wireframe origami or tiles. In addition, many wireframe or closely packed origami structures can be folded with higher concentrations of other cations (such as Na^+) instead of magnesium[70,71]. However, DNA origami structures synthesized in buffers with high Mg^{2+} concentrations may become structurally unstable when transferred into low-salt solutions[72].

DNA origami structures are folded via one-pot self-assembly[7,73,74]. TABLE 2 presents the best practices for working with the reagents necessary to create DNA origami. In general, to reduce non-specific aggregates, the concentration of staple strands is 10–20× higher than the concentration of scaffold strands. For dynamic DNA structures, the staples involved in dynamic reconfiguration are often purified by denaturing PAGE to ensure 100% incorporation of these important staples into the desired location in the structure. The staple to scaffold ratio for these staples is generally set as 1.5–2 (REF.[75]) to preferentially promote intramolecular over intermolecular interactions and should be optimized depending on the desired dynamic function. The mixture undergoes a thermal annealing process, in which it is heated to near boiling for a short time and then gradually cooled to allow spontaneous self-assembly of DNA origami[7,11,12,73]. The specific annealing procedure depends on the complexity of the DNA origami — small wireframe structures and 2D origami need a few hours, whereas multilayer 3D structures may require several days because the high degree of folding is less thermodynamically favoured. In addition, stepwise assembly may be involved for creation of structures integrated with other functional materials, or hierarchical structures as discussed below[74]. The ability to fold complex DNA nanostructures with 100% yield at a constant temperature would be valuable[76].

Hierarchical assembly. The construction of hierarchical assemblies made of origami units (also called super-origami) was first proposed by Rothemund and mainly based on canonical DNA hybridization[7]. Subsequent work demonstrating sticky end-based assembly of DNA origami tiles into 2D lattices has expanded the capacity to generate bottom-up pattern complexity[77], whereas lipid bilayer-assisted self-assembly has offered the possibility of fabricating supramolecular architectures in a micrometre space[78,79]. Recently, novel methods

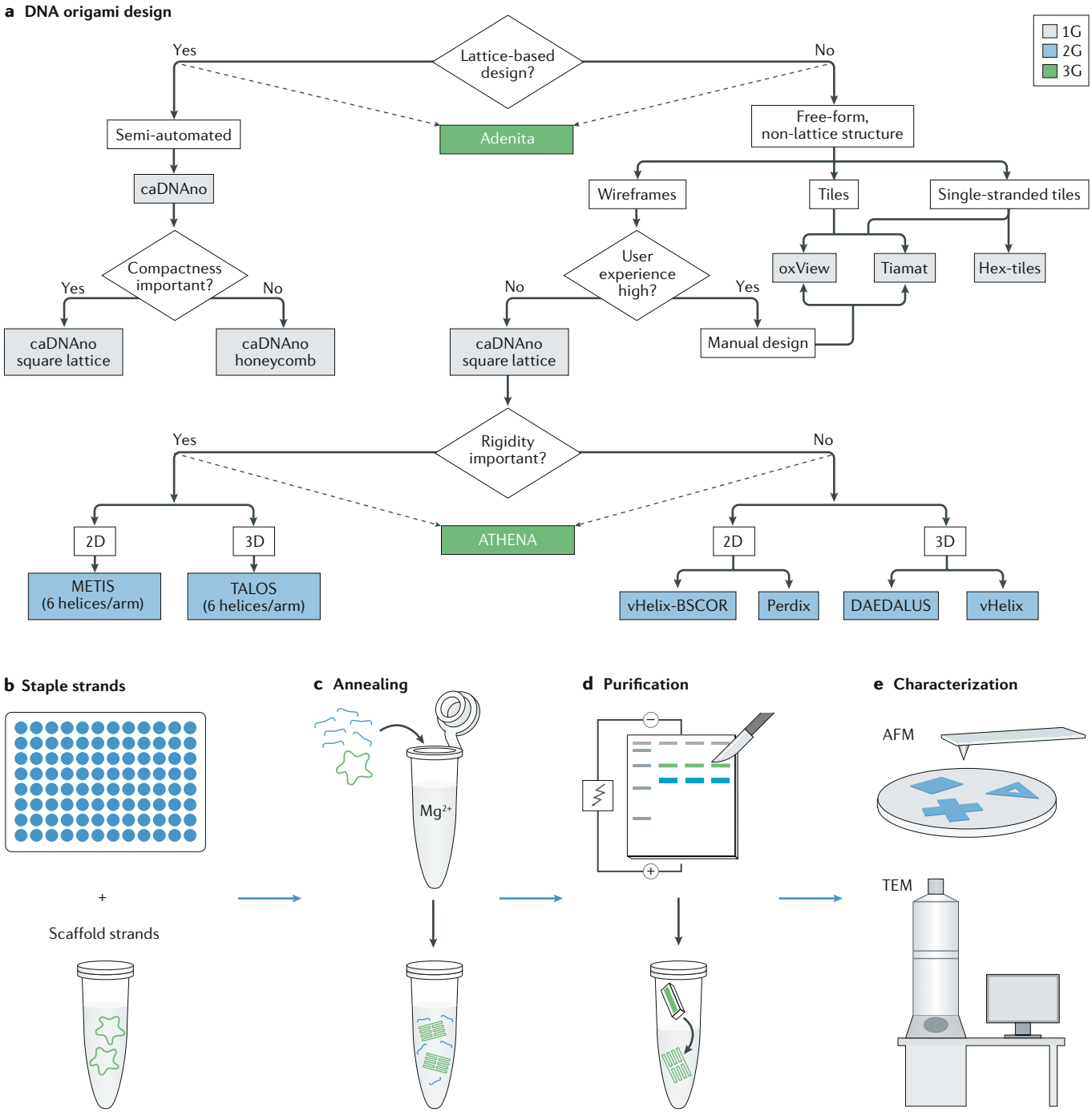

Fig. 2 | **General principle of DNA origami design and assembly. a** | DNA origami structures are usually designed using the software shown in the decision-making flow chart. The coloured boxes (grey, blue and green, design tools of the first (1G), second (2G) and third (3G) generation, respectively) represent the software that are best suitable for a given task. **b** | Staple strands are usually purchased commercially and stored in 96-well plates. Single-stranded viral DNA (usually from M13 bacteriophage) is typically used as a scaffold for DNA origami structures. **c** | The M13 scaffold mixed with staple strands (with a large excess) is assembled through thermal annealing in a saline buffer solution (typically with 12.5 mM Mg^{2+}). **d** | The structures are usually purified using agarose gel electrophoresis, with the excision of DNA bands from the gel and purification of the structure. **e** | Characterization is mainly done using atomic force microscopy (AFM), which observes 2D and single-layer origami structures, or transmission electron microscopy (TEM) to characterize 3D origami structures and multilayer structures.

Table 1 | **Comparison between different DNA origami design software**

Software	Ability	Advantages	Disadvantages
First-generation design software			
caDNAno[8]	Lattice-based (honeycomb or square) scaffolded DNA origami design	Simplest user interface among all first-generation design software Semi-manual inter-helix crossover creation Most widely used Strong community and developer support	Difficult to design 3D structures owing to the lack of a 3D interface with single-base resolution Difficulty of downstream design modification, for example single-stranded staple overhangs Not suitable for non-parallel helix based-structures such as 3D wireframes, single-stranded tiles, etc.
Tiamat[269]	DNA nanostructure design without lattice or scaffold limitations	Versatile Suitable for almost any structure, ranging from wireframes to single-stranded tiles, DNA crystal motifs, etc. Parallel, non-parallel and branched helix designs 3D workspace with single-base resolution Easy downstream design modifications Custom sequence generator with options to vary G-C%, unique sequence limit, G-repetition, etc. that can be used for other applications as well	Manual creations of crossovers Prerequisite knowledge required Less widely applied than caDNAno, when simple designs are needed Only Windows version, no macOS version available Weak community support
SARSE-DNA[14]	Lattice-based DNA origami design	Very similar to caDNAno Option to export as all-atom PDB format for molecular dynamics simulations	No parallel helix based-structures such as wireframes, single-stranded tiles, etc. Very similar to caDNAno for scaffolded origami designs
oxView	Web-based design platform designed for oxDNA	Completely web-based, hence minimal system requirements Very strong community support Additional option for coarse-grained molecular dynamics simulations with oxDNA	Not suitable to design large and complex structures such as wireframe or multilayered origami from scratch Web-based, hence requires to be operated online Offline mode is still in beta testing
Hex-Tiles[301]	Triangulated wireframe SST structures	SST-wireframe design Custom arrangement of sequences in 96-well plates according to experimental convenience Reusage of existing strands	Limited to SST structures Not used widely in the community
Second-generation design software			
vHelix[15]	Automated design of scaffolded 3D DNA origami with single–dual duplex edges	Automated design of complex 3D structures from user-drawn polygonal meshes No parallel helix required Only design platform with in-built relaxation algorithms to predict the folding of complex polyhedral structures The minimum use of DNA is ensured Cost-effective and low-salt stable structures	Polygonal wireframe structures must be topologically equivalent to a sphere, hence not suitable for simpler 1D, 2D structures or more complex 3D structures Rely on Autodesk Maya or other 3D design software to create the mesh design Different interface requirements for design, relaxation and sequence generation Relatively new, less widely tested across laboratories than caDNAno and Tiamat
DAEDALUS[47]	Automated design for scaffolded 3D DNA origami with dual duplex edges	Fully automated design without limitation to spherical topologies Less material consuming wireframe designs ensure cost-effective and low-salt stable structures	No graphical user interface, requires MATLAB to run No integrated relaxation algorithms to predict structure folding Each arm must contain at least two helices, hence more material-intensive than vHelix Edges must be multiples of 10.5 bp
TALOS[9]	Automated design for scaffolded 3D DNA origami with honeycomb six-helix edges	Automated design of mechanically stiff structures Control over distribution of staple lengths	Material-intensive and incompatible with low-salt, physiological buffers
Third-generation design software			
ATHENA[51]	Integrated platform incorporating features of DAEDALUS, PERDIX, TALOS and METIS	An integrated platform containing features of all second-generation software for wireframe origami design, hence 2D or 3D, more rigid or less rigid — any type of wireframes can be generated using a single software Can be integrated with caDNAno for custom sequence editing	Still not widely tested across laboratories Minimum number of helices per arm is still two, hence material-intensive

Table 1 Cont. | **Comparison between different DNA origami design software**

Software	Ability	Advantages	Disadvantages
Third-generation design software (cont.)			
Adenita[52]	–	Most versatile software to date for DNA origami design Contains almost all features of all first and second-generation software Only software that can accommodate biomolecules other than DNA within the design Very user-friendly GUI integrated with the SAMSON commercial nanoscale simulation software Options to import part of previously published structures to build on Option to predict folding by in-built molecular dynamics simulation tool makes it useful	Still not widely tested across laboratories The 3D wireframe design still uses the DAEDALUS algorithm, hence each arm of the wireframe structure contains at least two helices, making it material-intensive

have emerged for the predictable self-organization of origami shapes, making those structures excellent components for ordered assemblies of micrometre dimensions[20,21,26,74,80–82]. DNA origami structures exploit stacking[81], a kind of nucleobase interaction that takes advantage of the dense set of blunt ends at the edges of the structures. Such bases can establish base stacking interactions with exposed terminal bases at the boundaries of a different origami unit. The binding force between origami components can therefore be manipulated by the suitable choice of the number and base sequence of the edge–staples to promote geometric matching for maximal surface contact between facing edges. In other words, shape complementarity emerges as an additional factor for controlling the hierarchical assembly of DNA origami architectures[20,26,80,81].

Purification. Purification and enrichment are crucial steps to use DNA origami structures for optical/electronic and biochemical/biomedical applications, especially when the structures require site-specific functionalization. The quality and purity of DNA origami structures can be assessed with agarose gel electrophoresis owing to the difference in gel migration rates[17] between correct products and by-products. A detailed overview of the purification methods has been covered elsewhere[46] and is beyond the scope of this Primer. Commonly used purification methods include gel purification[83], ultrafiltration[84], polyethylene glycol (PEG) precipitation[85], ultracentrifugation[86] and size-exclusion chromatography[46]. Depending on the application, the optimal purification method should be chosen by comparing quantitative (yield, duration) and qualitative (volume limitation, dilution, residuals, damage) measures[73]. For example, PEG precipitation promotes a high yield of the target species but also introduces residual PEG molecules; filter purification with molecular weight cut-off membranes provides residual-free separation but is limited in volume and may lead to non-specific aggregation in some cases; and gel purification is suitable for bandpass molecular weight separation, for example to separate modified DNA origami structures and the unbound moieties, but its yield is low and this method generally introduces agarose and ethidium bromide contaminants (FIG. 2d).

Results

In this section, we provide typical characterization data of DNA origami assemblies using ensemble and single-molecule techniques (TABLE 3). These techniques can inform users about the self-assembly process by providing information such as the yield and correct formation of the target structure, and the fraction of side products present, including high-molecular weight aggregates and misfolded and partially assembled intermediates.

Ensemble characterization. The first piece of information needed on the self-assembly process is whether it succeeded and to what extent. To this end, the assembly mixture is analysed with ensemble methods such as gel electrophoresis, UV–visible and fluorescence spectroscopy, and circular dichroism. These techniques provide the average chemical or physical characteristics of the bulk of the molecules in solution, as they are able to discern between groups of molecules with similar properties but unable to pick out individual molecules. The outcome of the assembly reaction is examined in terms of populations of end products whose molecular details are unknown.

Gel electrophoresis is the method of choice to assess self-assembly performance[17,69,70,76]. Upon application of an electric field, DNA molecules migrate along a polymer gel matrix according to their size, charge and shape, enabling the separation of multimers of different orders as well as misfolded and/or partially assembled intermediates (FIG. 3a). DNA is then visualized by staining the gel with an intercalating UV-fluorescent dye, and products are quantified using fluorescence gel scanners and modern software tools. Alternatively, identification and isolation of the product of interest can be done using fluorescent dyes[84]. These are incorporated into the DNA nanostructure, substituting selected staple strands of the origami assembly mixture with their fluorescently modified analogues, commercially available in different forms at an affordable price. When combined, gel electrophoresis and fluorescent probes can be used to check the extent of staple incorporation and hybridization defects[87]. Besides their use as markers, photoactive compounds capable of Förster

Table 2 | **Best practices for working with the reagents necessary to create DNA origami**[46,74,264]

Component	Best practices
Scaffold	When designing an origami structure, consume as much scaffold as possible
	Keep the unused scaffold part no bigger than 100–200 nucleotides at one end of the desired structure
	Keep scaffold frozen at –20 or –80 °C as small aliquots
	Avoid frequent freeze–thaw
Staples	Order in 96-well plates
	Store plates at 4 °C for short-term storage, –20 or –80 °C for long-term storage
	Avoid frequent freeze–thaw
	Purify important staples by denaturing PAGE or high-performance liquid chromatography, ensuring perfect incorporation of the strands into the origami
	Order modified staples separately from normal unmodified staples, making it convenient to anneal the structures
	Staple mixes can be created for different parts of the origami for frequent annealing, avoiding the need to repeatedly freeze–thaw the source plates
Folding buffer	Use freshly prepared buffers
	For buffers to be used for sensitive microscopic techniques such as atomic force microscopy or transmission electron microscopy, filter the buffers using syringe filters and store them in glass vials, which avoids leaching of plastic fibres

resonance energy transfer (FRET) can be employed to monitor dynamic processes of structural reconfiguration in real time[12,88–92] (FIG. 3b–d). Indeed, as the number and distance among the fluorophores in the final construct are fully predictable, any structural transformation that implies a change in their spatial configuration can be monitored and quantified by FRET spectroscopy, allowing, for example, insights into the thermodynamics of the self-assembly process or the kinetics of isothermal transformations[26].

Less commonly, UV–visible and circular dichroism spectroscopy have also been used to characterize ensemble optical properties of DNA assemblies modified with metal nanoparticles. UV–visible spectroscopy has been used to measure DNA concentration-dependent properties[93], whereas circular dichroism spectroscopy has typically been employed to identify the chiral signature of the final compound[94].

In general, ensemble techniques are valuable tools to gather a global picture of the assembly process, where their focus is to quantify the fraction of the target structure obtained compared with the side products through the characterization of an average chemical–physical property of interest. Their major limitation is a lack of sufficient spatial–temporal detail. For such purpose, single-molecule techniques are instead preferable.

Single-molecule characterization. The main feature of a DNA origami structure is to provide a molecular surface where desired chemical species can be positioned at predictable nanometre distances. As each nucleobase of the DNA object can be chemically functionalized, this would in principle enable the positioning of two distinct molecules along two consecutive bases on the same helix, resulting in a spacing of only 0.34 nm along the helical axis. In practice, point modifications are separated by at least one and a half helical turns (ca. 5.4 nm) to allow easier identification with standard single-molecule techniques (although recent developments enable reaching sub-5-nm resolution). Both force and optical-based methods have been employed to characterize the structure and function of DNA origami objects[95–97], such as atomic force microscopy (AFM), transmission electron microscopy (TEM), cryo-EM, single-molecule fluorescence microscopy and, more recently, single-molecule force measurements.

The very beginning of the DNA origami era was associated with eye-catching AFM images that clearly demonstrated the success of the method and spurred on further research[7] (FIG. 3e). By sensing the intermolecular forces occurring between the tip and the sample, AFM provides the height profile of the specimen deposited on an atomically flat surface — its detailed topographical map — with a lateral resolution of 1–2 nm. The capability of this technique to reveal fine structural features has recently been employed to better understand the folding pathway of planar DNA origami structures by providing accurate wide-field images of hierarchically self-assembled constructions[11,81,98–100] (FIG. 3f). Modern AFM instruments also combine high spatial resolution with a temporal resolution of seconds to sub-seconds[95], sufficient to monitor topological changes in single molecules[101] (FIG. 3g) or DNA processing events in real time[102,103]. Although AFM is a powerful tool to characterize 1D and 2D structures, it may not be suitable for the imaging of 3D or multilayer DNA origami because the deformation caused by the AFM tip during scanning makes it difficult to obtain the complete topography of surface features in low-rigidity structures.

For the characterization of 3D DNA objects, TEM and cryo-EM are preferred instead. Uranyl formate or other uranyl salts are commonly used to produce negative stain contrast in TEM micrographs because they are excluded from the densely packed DNA structures. The result is a bright and fine-grained image of the specimen on a dark background. Image processing (for example, using EMAN2 software) can be used to assess the heterogeneity of DNA origami, identify structural flaws and

reconstruct 3D models from TEM images of a single structure.

The first TEM images of 3D DNA origami structures showed the suitability of this technique to reveal the successful formation of the intended space-filled architectures[17,18] (FIG. 3h). However, the high vacuum and dehydration conditions associated with TEM imaging may result in flattening and distortion of structures that display inner cavities. In such instances, electron microscopy imaging in fully hydrated cryogenic conditions is preferred, as it ensures structure preservation and enables observation of the macromolecule in the close to native state in solution. Using cryo-EM, the first pseudo-atomic model of a 3D DNA object was obtained

Table 3 | **Comparison of different structural analysis methods and best practices**

Method	Advantages	Disadvantages	Best practices
Gel electrophoresis	Much simpler and resource-friendly compared with microscopic methods Provides bulk estimation about the yield of structure formation, its purity and reconfiguration Allows extraction of the desired sample population	Cannot provide in-depth structural insights at the single-molecule level	Casting and running gel buffers and sample buffer should ideally be identical Gels should run at 0–4 °C to prevent melting and sample degradation Running buffer should not contain more than 100 mM monovalent ions Intercalating dyes tend to fall off after 2–3 h; if longer gel running times are needed, either perform staining after gel migration or use fluorescently labelled strands Intercalating dyes should be avoided if the structure will be gel-extracted for high-resolution studies; in this case, visualization of the DNA by fluorescent labels or UV shadowing is preferred UV shadowing can be used to visualize unlabelled, unstained complexes by placing the gel over a silica gel bed where the DNA would look dark blue and the rest of the gel would look green; the amount of DNA to be loaded and the position of the band must be optimized by the user depending on the structure and application
Fluorescence spectroscopy	Highly sensitive Provides distance-dependent information when applied to FRET fluorophore pairs Can be used to monitor dynamic events in real time	Requires fluorescent modified strands (expensive) Structural information is related to the local dye's environment	Fluorescently modified oligomers should be checked for purity to ensure full incorporation of the desired dyes into the structure Accurately prepare control donor-only samples for reliable quantification of the FRET effect Cyanine, Alexa or Atto dyes are preferred over fluoresceine or rhodamine dyes owing to their higher photostability and wider choice of excitation/emission wavelengths
AFM	High fidelity Lateral resolution up to ca. 1–2 nm Imaging can be done in fluid or in air Modified AFM tips can be used to study the mechanical and elastic properties of the DNA High-speed AFM can probe structural dynamics in real time	Unsuitable for 3D or multilayer DNA structures Time-consuming	Nickel acetate can be used to fix the DNA sample on the mica surface; the amount of Ni^{2+} should be carefully adjusted for origami type — smaller structures need higher [Ni^{2+}] to be immobilized on surfaces Purified samples give best results Use deionized water to get rid of salts when performing in air Tapping mode with SNL-10 or BL-AC40TS-C2 tips is recommended Use ScanAsyst mode for best imaging results
Transmission electron microscopy	Best for 3D structures Highest resolution Can be coupled with particle averaging methods to enhance resolution Especially suitable for metal nanoparticle modified structures	Negative staining is cumbersome and time-consuming Difficult to obtain sample height information Structural deformation due to drying	Transmission electron microscopy grid should be discharged to enhance hydrophilicity Before staining, add NaOH solution to adjust the pH of the uranyl formate solution EMAN2 software can be used to assess the heterogeneity of DNA origami
Single-molecule force measurements	Detects molecular forces with piconewton resolution Allows detection of rare dynamic events (for example, conformational changes, formation and disruption of bond)	Highly specialized technique Might be cumbersome for non-experts Data analysis requires good mathematical and biophysical skills	A dual optical tweezer is the preferred instrumental configuration to measure structural changes of the trapped DNA Long (ca. 3,000 bp) tethers are recommended to trap the sample Use appropriate controls to understand the contributions to the force–extension curve

AFM, atomic force microscopy; FRET, Förster resonance energy transfer.

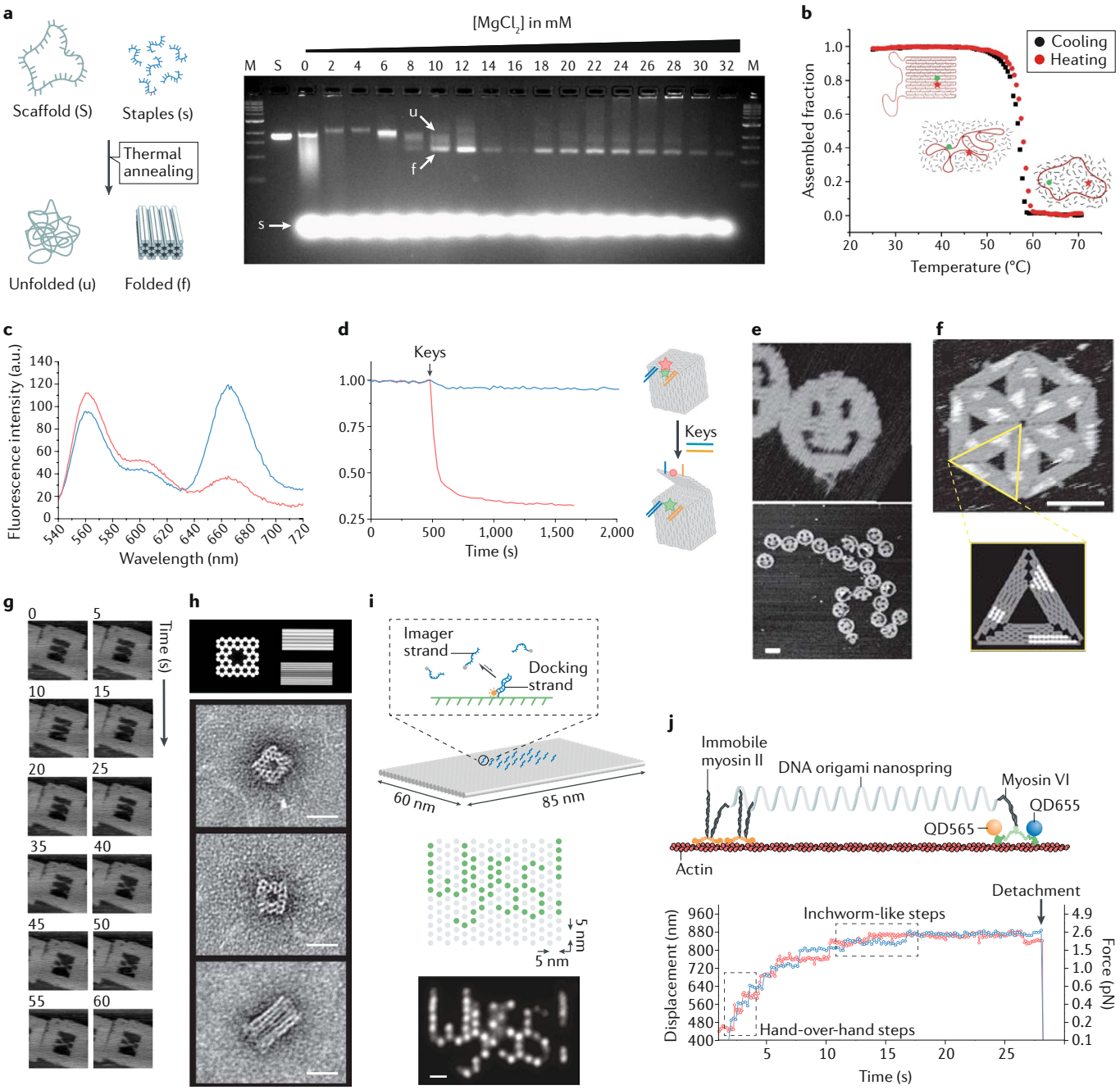

Fig. 3 | **Representative examples of ensemble and single-molecule characterizations of DNA origami structures. a** | Agarose gel electrophoresis of the self-assembly products obtained at increasing magnesium ion concentrations (from 0 to 32 mM)[70]. **b** | Thermal-dependent Förster resonance energy transfer (FRET) measurement of the assembly and disassembly of DNA origami microdomains (green and red dots indicate, respectively, a fluorescein and a TAMRA molecule)[92]. **c** | Ensemble FRET measurements of a closed DNA box before (blue curve) and after (red curve) the addition of keys[89]. **d** | Kinetics of lid opening monitored by the change in emission of the donor (red curve) upon addition of key oligonucleotides (black arrow) or an unrelated oligonucleotide (blue curve). Initial fluorescence was normalized to one. Schematic of the process indicated in the right panel[89] (blue and orange lines, lock and key strands; pink and green stars, fluorescent emission from Cy5 and Cy3 labelling; red circle, Cy5 lost emission). **e** | First atomic force microscopy (AFM) images of quasi-planar DNA origami structures[7]. Scale bar is 100 nm. **f** | AFM imaging of hierarchical DNA assemblies decorated with bulky molecules at predictable positions (shown as white sections)[7]. Scale bar is 100 nm. **g** | Topological reconfiguration of G-quadruplex motifs imaged for 60 s at 5-s intervals using fast-scanning AFM[101]. Image size is 160 nm × 160 nm. **h** | First electron microscope characterization of a space-filled 3D DNA origami structure under different perspectives[17]. Scale bars are 20 nm. **i** | DNA-based point accumulation for imaging in nanoscale topography (DNA-PAINT) super-resolution imaging of a DNA origami structure[106] relies on the transient binding between a dye-conjugated imager strand (blue) and a docking strand (at the centre of the structure). Schematics of a 'Wyss!' pattern on a DNA origami surface with 5-nm pixel size (each green dot indicates a docking strand) and resulting single-particle class average ($n = 85$)[302]. Scale bar is 10 nm. **j** | Coupled single-molecule force spectroscopy/optical measurements of the stepping behaviour of myosin VI when tethered to an optically trapped DNA origami nanospring[115]. Part **a** adapted from REF.[70], CC BY 3.0 (http://creativecommons.org/licenses/by/3.0). Part **b** adapted with permission from REF.[92], ACS. Parts **c** and **d** adapted from REF.[89], Springer Nature Limited. Parts **e** and **f** adapted from REF.[7], Springer Nature Limited. Part **g** adapted with permission from REF.[101], ACS. Part **h** adapted from REF.[17], Springer Nature Limited. Part **i** adapted from REF.[302], Springer Nature Limited. Part **j** adapted from REF.[115], CC BY 4.0 (https://creativecommons.org/licenses/by/4.0/).

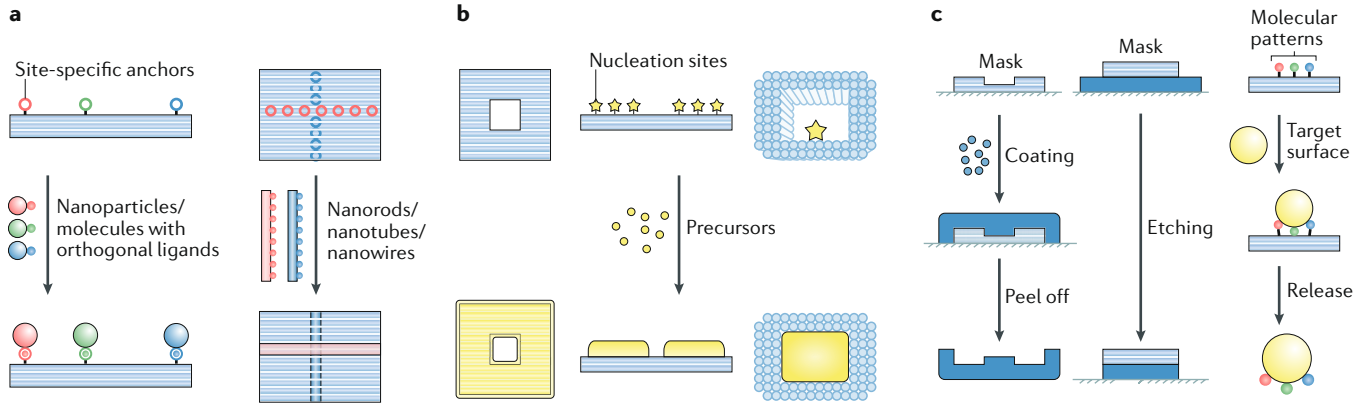

Fig. 4 | **Typical approaches of DNA origami-based nanofabrication. a** | Site-specific assembly. The site-specific anchors on DNA origami templates enable spatial arrangement of nanoparticles/molecules or nanorods/nanotubes/nanowires with prescribed species, numbers and orientations[32,118]. **b** | In situ synthesis. DNA origami templates mediate the adsorption/reaction of certain precursors on their surface or in their cavities[16,28,129]. **c** | Nanolithography. DNA origami structures as masks or stamps enable the transfer of their shapes or molecular patterns to other materials[33,135,137].

with an overall resolution of 11.5 Å, confirming the formation of a structure with the expected topology[104]. Although the structural information gathered by raw individual electron microscopy images is relatively low, acquiring large sets of individual particle images and processing them semi-automatically using sophisticated post-imaging software tools results in a dramatic increase of the signal to noise ratio and, in most cases, leads to full reconstruction of the 3D structure with near-atomic resolution. TEM provides images of the specimen with a wide field of view and has successfully been used to characterize the formation of micrometre-large DNA origami hierarchical assemblies obtained by base stacking, guided hybridization or a combination of both[20,82]. Finally, although TEM has a lower time resolution, it can still be used to distinguish changes in structurally distinct states upon environmental changes in pH, salt concentration or temperature, and has revealed the triggered dynamics of molecular machines[26].

Fluorescence-based techniques provide an indirect characterization of local molecular events occurring near dye molecules that are attached to the DNA surface using various bioconjugation methods. As the DNA objects are typically smaller than the diffraction limit of light (ca. 200 nm), their resolution by ordinary fluorescence imaging is limited. This has changed with the advent of single-molecule FRET and super-resolution microscopy. Whereas FRET relies on the distance-dependent energy transfer between a donor and an acceptor photoactive probe, the basic principle behind super-resolution imaging is the consecutive switching of fluorescent molecules between an 'on' and 'off' state. Stochastic reconstruction methods, such as point accumulation for imaging in nanoscale topography (PAINT)[97,105], have been combined with the transient binding of short fluorescent DNA strands (DNA-PAINT) for the direct observation of dynamic events on DNA origami scaffolds[106,107] (FIG. 3i). In general, single-molecule fluorescence techniques have been successfully implemented to describe local dynamic events and quantify distance-dependent molecular interactions, conformational dynamics and kinetics of diffusion processes[108–111].

Finally, although still limited in its use, single-molecule force spectroscopy based on optical tweezers is a promising application. This technically challenging method has already been employed to observe the unzipping of small DNA origami domains[99,112,113] and the kinetics of G-quadruplex unfolding within a DNA origami cavity[114]. Particularly when in combination with optical methods[115], this method promises to be an essential tool for the investigation of dynamic events at the single-molecule level (FIG. 3j).

Applications

With proper chemical modification at specific locations, DNA origami structures provide a versatile engineering platform where nanoscale entities — from small-molecule dyes to massive protein complexes, inorganic nanowires and 3D liposomes — can be manipulated in a highly programmable manner. Prominent examples include nanomaterial fabrication that relies on precise control of molecular placement, as well as the study of biological processes resulting from well-organized molecular assemblies. In this section, we review selected DNA origami-based applications in materials science, physics, engineering and biology, with the hope that these developments of the past decade may offer a sneak peek into the technology's future impact.

Nanofabrication. Owing to their highly customizable geometric properties, such as size and shape, and their nanometre resolution, DNA origami structures have been used as templates or frameworks for the assembly or synthesis of diverse materials with nanometre precision. They have shown great promise in the nanofabrication of inorganic (metallic or non-metallic), polymeric and biomolecular assemblies and patterns, with enhanced structural stability and/or desired physicochemical properties[6,27,74,116]. Importantly, DNA origami-based approaches allow massive parallel fabrication (for example, 10^{12} copies of products in a single operation)[6] either in solution or on a surface.

A representative nanofabrication approach (FIG. 4a) employs DNA origami templates with site-specific

anchors (typically the staples or their appendices) to attach other prefabricated nanomaterials via user-defined specific interactions. This approach generates a highly programmable arrangement of atomic-scale discrete nanostructures such as nanoassemblies in solution (colloids) or on a surface (patterns), metal and semiconductor nanoparticle assemblies with prescribed heterogeneity, anisotropy and/or chirality[117–121], and carbon nanotubes with defined alignments[32,122,123]. Further packing or assembly can then generate higher ordered 2D patterns[124] or 3D superlattices[125,126]. In addition, the programmable reconfigurability of DNA origami allows nanoassemblies to be dynamically rearranged and creates tuneable physicochemical properties responsive to environmental stimuli[31,120,127].

During in-situ synthesis (FIG. 4b), precursors in solution (for example, metal ions, silicification precursors or lipid molecules) adsorb/react/deposit on DNA origami templates with or without prescribed nucleation sites[128–132] and generate continuous architectures shaped by the morphologies of the templates or their cavities[16,133]. This approach promotes nanoarchitectures with almost arbitrary, user-defined geometries in solution or on a surface[28,131,132,134].

DNA origami structures and their derivatives have also been employed as masks or stamps for nanolithography (FIG. 4c), enabling high-fidelity transfer of prescribed 2D nanoscale patterns onto other 2D or 3D materials[33,135–137]. In this way, the size and shape of 2D nanomaterials such as graphene can be precisely tailored for the fabrication of diverse electronic devices with nanometre resolution. In addition, the combination of traditional lithography and DNA origami-enabled site-specific assembly has facilitated large areas of spatially ordered arrays of functional nanoparticles and molecules on surfaces[138–140].

Nanophotonics and nanoelectronics. Attractive optical and electronic properties arise from structural features with dimensions below the electromagnetic wavelengths (typically <100 nm). However, precise sculpting of materials at that scale is challenging. DNA origami-templated nanostructures with high structural programmability at the nanometre level allow tailorable optical or electronic properties, including tuneable conductivity, plasmon coupling, Fano resonances and plasmonic chirality, and hold great promise for applications in nanophotonics and nanoelectronics[31,141].

Owing to localized surface plasmon resonance, the photonic properties of complex metal nanostructures composed of multiple nanoparticles are dependent on particle size, shape and the interparticle spacing and configuration. Rigid DNA origami templates enable precise arrangement of heterogeneous plasmonic nanoparticles, such as the coupling of large-size AuNP and AgNP (>40 nm)[142], as well as small interparticle spaces (for example, sub-5 nm) with little variability[143]. This leads to prominent and predictable plasmon coupling and Fano resonances[142] suitable for studying nanoplasmonic effects. A DNA origami-templated multi-particle plasmon coupling chain showed ultra-fast and low-dissipation energy transfer, exemplifying a new route to plasmonic waveguides[144,145]. In addition, DNA origami-based nanofabrication enables complex asymmetrical plasmonic nanoparticle assemblies[44,118,120,146–152] with structural chirality and strong plasmon coupling. These properties interact differently with left and right circularly polarized light, leading to pronounced circular dichroism in the visible spectrum (FIG. 5a).

By organizing multiple chromophores/fluorophores with distinct spectral properties, prescribed distances, orientations and/or donor to acceptor ratios, DNA origami platforms enable efficient light-harvesting antennas and photonic wires with long-range directional energy transfer[35,36,153,154]. Precise positioning of Raman chromophores or fluorophores between plasmonic nanoparticles can generate quantitative surface-enhanced Raman spectroscopic[142,155] or fluorescence spectroscopic responses[156,157] (FIG. 5b), which provide promising materials for single-molecule sensing when coupled to target-specific ligands and trigger-responsive dynamic DNA self-assemblies. Precise placement of fluorophore-labelled DNA origami onto lithographically patterned photonic crystal cavities allows engineering of their coupling and thereby digitally controllable cavity emission intensity[139] (FIG. 5c).

Finally, DNA origami allows shaping and arrangement of diverse materials with different conductive/semiconductive/dielectric properties and provides a new fabrication route for complex nanoelectronic modules and devices, such as nanowires with tuneable conductivity[133], field-effect transistors based on spatially organized carbon nanotubes[32,158] (FIG. 5d) or DNA-templated graphene nanoribbons[33] (FIG. 5e).

Catalysis. Biocatalytic transformations are central to the production of metabolites, biomolecules and energy conversion in living systems. In very early DNA nanotechnology considerations, Seeman envisioned DNA structures with the potential to organize proteins in spatially well-defined patterns for structural analysis[1]. Today, we have realized that DNA nanostructures offer an excellent platform for spatially organizing enzymes owing to the unique addressability of DNA origami[159].

The hypothesis motivating spatial organization of enzymes in reaction cascades is that the diffusion of small-molecule substrates between enzymes is proximity-dependent, and thereby the rate of the cascade is also proximity-dependent. The most common strategy for organizing enzymes (and proteins in general) in DNA nanostructures is to conjugate an oligonucleotide strand to each enzyme separately, by one of the many available methods for protein–DNA conjugation[116]. The DNA structure is designed with complementary single-stranded domains extending from the positions where the individual proteins in the cascade will be located, and subsequent addition of the DNA–protein conjugates attaches the conjugates to the DNA structure in the desired positions by hybridization[160–164]. The proximity hypothesis was challenged in a recent study, which argued that the negatively charged DNA structures to which the enzymes are anchored alter the local pH in favour of catalytic processes[165]. This argument cannot account for all of the proximity effects

observed experimentally, however, and uncertainty about the proximity effect remains[163,166].

In the studies above, the enzymes are confined in one or two dimensions. Another strategy is to confine enzymes in three dimensions to potentially enhance both the channelling of intermediates and the impact of the origami structure on the enzyme. In some examples, single proteins have been encapsulated in 3D origami

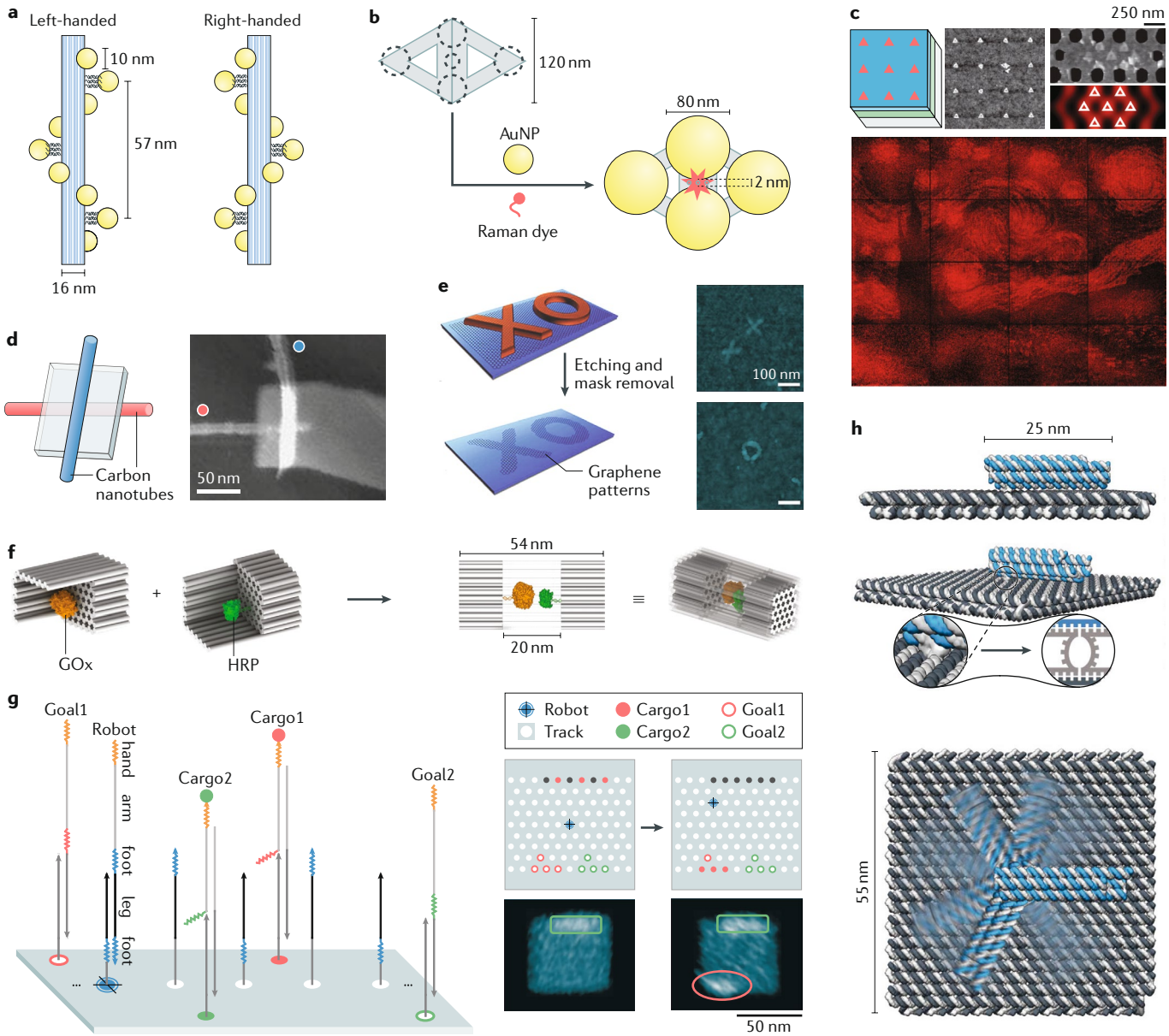

Fig. 5 | **Application examples in nanophotonics and nanoelectronics, catalysis, computation and molecular machines. a** | Left and right-handed AuNP nanohelices organized by DNA origami, which exhibit mirror symmetrical circular dichroism signals at visible wavelengths[118]. **b** | Raman dye molecules placed precisely in the gap among the AuNPs on DNA origami, presenting single-molecule surface-enhanced Raman spectroscopy[142]. **c** | Engineering photonic crystal cavity emission via precision placement of DNA origami[139], enabling the creation of an image with 65,536 pixels (Vincent van Gogh's painting *The Starry Night*). **d**,**e** | Schematic and atomic force microscopy (AFM) images of vertically crossed carbon nanotubes (coloured red and blue) arranged by DNA origami[32] (part **d**) and tailored graphene patterns resulted from nanolithography with metallized DNA origami structures as masks[33] (part **e**), enabling field-effect transistor application. **f** | An enzyme couple, glucose oxidase (GOx) and horseradish peroxidase (HRP), encapsulated in the cavity of a DNA origami nanocage. Their spatial proximity in the confined environment enable enhanced cascaded catalytic activity[109]. **g** | A cargo-sorting robot on DNA origami that can transport cargos (Cargo1 and Cargo2, marked with red or green solid circles) to specified locations (Goal1 and Goal2, marked with red or green hollow circles) via toehold (coloured arrows)-mediated strand displacement reactions. The results visualized by AFM[42] show cargo transfer from the initial locations (boxed) to the goal locations (circled). **h** | A DNA robotic arm driven by an electric field[110]. Upper to lower: side view, perspective view (with a close-up showing the flexible joint) and top view of the robotic arm (blue striped) that can rotate on the platform (grey striped). Part **a** adapted from REF.[118], Springer Nature Limited. Part **b** modified from REF.[142], Fang et al., *Sci. Adv.* 2019;**5**: eaau4506. © The Authors, some rights reserved; exclusive licensee American Association for the Advancement of Science. Distributed under a CC BY-NC license. http://creativecommons.org/licenses/by-nc/4.0/. Part **c** adapted from REF.[139], Springer Nature Limited. Part **d** adapted from REF.[32], Springer Nature Limited. Part **e** adapted from REF.[33], Springer Nature Limited. Part **f** adapted from REF.[109], CC BY 4.0 (https://creativecommons.org/licenses/by/4.0/). Part **g** adapted with permission from REF.[42], AAAS. Part **h** adapted with permission from REF.[110], AAAS.

structures[90,167,168], whereas other cases have demonstrated encapsulation of enzyme couples (for example, glucose oxidase and horseradish peroxidase)[109,169,170], forming enzyme cascades in DNA origami nanostructures such as a flat origami sheet[169], an open-ended honeycomb-lattice DNA origami tube[170] and a closed honeycomb lattice nanocage[109] (FIG. 5f). In all three cases, both significant rate enhancement of the enzyme cascade and higher enzyme stability were observed[171].

Computation. DNA is an information-carrying molecule with a high degree of thermodynamic and kinetic programmability because the rate of its toehold-mediated strand displacement reactions can be tuned[25,37]. Rational sequence design thus enables the formulation of both potential binding events in a DNA-based system and when and in what order these events must occur. Owing to these properties, DNA is a popular substrate for in vitro signalling networks and molecular computation, starting with Adleman's implementation of the travelling salesman problem[172]. Rational sequence design — often the last step in multiple layers of abstraction[173] — finalizes the encoded algorithm and optimizes the emergent physical behaviour of DNA-based circuits. This principle of abstraction is also present in structural DNA nanotechnology. For instance, the CaDNAno design process is mostly sequence-independent, as it happens on a higher abstraction level. Compatible base sequences that allow the design to be physically implemented are generated only in the final step. The key distinction, however, is that, instead of structural blueprints, the base sequences in DNA computation encode algorithms — instructions on the propagation of cause and effect through binding events. This has resulted in the embedding of intricate programs into mixtures of DNA molecules, such as Winfree's square-root calculator[174]. However, the scaling and computation speed of these diffusive circuits is limited by their lack of spatial organization[174].

DNA origami structures therefore provide a framework for scaffolding, co-localizing and compartmentalizing circuit components[175]. Spatial organization of DNA-based circuits through the use of origami frameworks can be exploited to accelerate reaction rates[176], modulate stochiometry[175], restrict or promote specific pathways[177,178] and outputs[179], compartmentalize distinct functional modules (for example, sensing, computation and actuation)[180], decrease computation errors stemming from crosstalk and increase sequence recyclability[176]. Furthermore, owing to improved physiological stability over small ssDNA and dsDNA, structural DNA nanotechnology could open doors for in vivo computation, including the rewiring of cellular signalling pathways[41,181].

Although localization mostly presents an optimization strategy for deterministic circuits, it enables entirely novel properties to emerge in systems that rely on stochastic methods. For instance, a DNA origami robot was designed that sorts unordered cargo into distinct piles, the algorithm of which relies entirely on a random walk and localized targets[42] (FIG. 5g). Similarly, random walkers can be guided by their local landscape[108]. In another application, Chao et al. implemented a parallel depth-first search algorithm to solve mazes on DNA origami sheets based on randomly searching DNA navigators[43]. Other recent developments in DNA computing seek to use structural reconfiguration or even the assembly itself as a computational architecture[100,182]. Alternatively, the results from DNA-based combinatorial selection can be localized on DNA origami structures, thereby coupling unique structural patterns to specific input signals[183]. Such applications would not be possible without spatial organization.

Molecular machines. The structural stability of DNA origami relies mostly on Watson–Crick base pairing and base stacking, both of which are reversible non-covalent interactions. Such reversibility has been exploited as a conscious design choice; for instance, a nanocontainer that opens and closes has more applications than one that only encapsulates[90,184]. Among other strategies, simply leaving parts of the scaffold or staple strands as single strands readily introduces flexible and reactive domains into the origami structure, for example via toehold-mediated strand displacement. The challenging aspect is how to reliably navigate the resulting conformational state expansion. Over the past decade, there has been an influx of dynamic DNA origami devices that transition between two or more (semi-)stable states[185]. Dynamic DNA structures differ in the type of input trigger as well as in the number of accessible states, their actuation speed and whether transitions are reversible[186]. One approach, for example, is to use the intrinsic electric properties of DNA, such as the negative charges on the DNA backbone[187], to fabricate an electrically controlled rotating arm that reversibly explores a continuum of states with only milliseconds of actuation time[110,188,189] (FIG. 5h). Many of these devices combine the rigidity of dsDNA with flexible single-stranded domains in order to achieve a dynamic function. Alternatively, domains can be mechanically interlocked to sterically direct their motion[190]. A major goal for DNA nanotechnology is to create molecular machinery and motors that do not just switch between states upon sensing some external change but also are progressively fuelled through a closed state path and generate change externally[191,192]. This change can be in the form of potential energy (for example, by establishing new chemical bonds) or kinetic energy (for example, by rupturing chemical bonds or by translocation). In order to fabricate such machines, it will arguably be necessary to integrate multiple simpler devices, in the same way as different functional parts are combined to create macroscale machines[185]. This includes expanding the chemical scope beyond that of base pairing and stacking, for instance through the inclusion of proteins. A recent study combines RNase-based catalytic walkers with steric direction of a DNA nanostructure, where the resulting system converts potential energy from RNA-based fuel into the unidirectional microscale movement of an origami roller[193]. Notably, this motor moves autonomously and without the aid of any external gradient or patterning.

Drug delivery. Exploiting DNA origami structures as carriers for drug delivery has garnered much interest[39]. First, as a natural biomaterial, DNA is biodegradable and

Enzyme cascades
Groups of enzymes in which the reaction product of one enzyme is the substrate for the next.

Abstraction
The translation of concrete DNA reactions into abstracted algorithms and instructions. By this method, the complex details are hidden from the persons operating the computing systems.

In vivo computation
Molecular computation implemented in living organisms, whose inputs/outputs are often interfaced with biological pathways/functions.

DNA origami robot
A molecular machine made by DNA origami that can autonomously perform specified task(s) with precise motions at the nanoscale.

shows little cytotoxicity[194,195]. Second, diverse therapeutic molecules and materials, including doxorubicin[194,196,197], immunostimulatory nucleic acids[198,199], small interfering RNAs[200], antibodies[184], enzymes[40] and so on, can be readily loaded onto the carriers via various interactions such as intercalation, base pairing or covalent binding[116] (FIG. 6a). DNA origami structures can also serve as containers with docking sites in their interior or within dedicated cavities, protecting the payloads from the environment and the environment from the payloads.

One outstanding challenge for drug delivery is to efficiently cross biological barriers to reach the drug targets with minimal off-target effects[201]. Previous studies have shown that well-folded DNA nanostructures are more resistant to enzymatic degradation[202] than ssDNAs/dsDNAs and are capable of entering live mammalian cells through energy-dependent endocytic pathways in an analogous way to some viral particles[203–206]. They can even cross cell walls in mature plants[207,208]. The dependency of cellular uptake on size and shape has also been investigated using DNA origami[209,210]. At the animal level, DNA origami structures are found to passively accumulate in solid tumours owing to enhanced permeability and the retention effect, enabling tumour-targeting drug delivery[194]. In addition, DNA nanostructures can penetrate mouse or human skin, suggesting applications in transdermal drug delivery to melanoma tumours[211]. Recently, DNA origami structures were found to preferentially accumulate in the kidney of a mouse, showing potential for treating kidney injuries[195] (FIG. 6b). As these in vivo distribution tendencies are believed to correlate to the dimensions of materials[212], the high structural customizability and monodispersity of DNA origami structures make it possible for them to selectively cross certain biological barriers; meanwhile, they can be retained elsewhere, enabling controllable distribution that is advantageous in these delivery studies.

To endow DNA nanostructures with active targeting ability, certain ligand molecules[201,213,214] with known receptors expressed on target cells have been incorporated into DNA origami carriers. Owing to the addressability of DNA nanostructures, the species, numbers, density and orientation of these ligands can be precisely defined, allowing optimized cell targeting ability based on spatial pattern recognition by the cells[201].

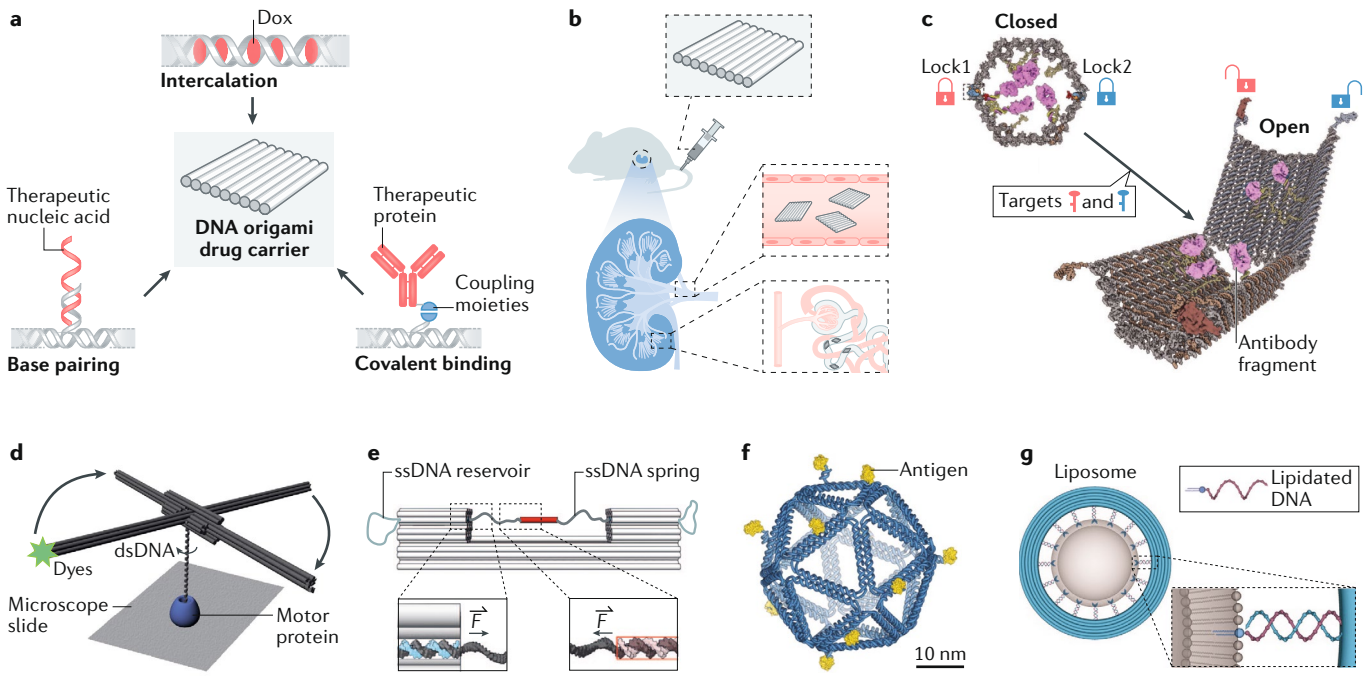

Fig. 6 | **Application examples in drug delivery, bioimaging and biophysics. a** | Representative drug loading strategies for DNA origami carriers, on the basis of DNA intercalation, such as intercalating for Dox delivery[194,196,197], base pairing for delivery of therapeutic nucleic acids such as immunostimulatory nucleic acids[198] and small interfering RNAs[200], and covalent binding, such as HyNic/4FB coupling for antibody fragments[184]. **b** | Preferential renal uptake of DNA origami enables the treatment of acute kidney injury[195]. **c** | A logic-gated DNA nanorobot locked with two different aptamer motifs (red and blue locks) that can be opened in the presence of both target molecules (red and blue keys) on the cell surface and expose the antibody fragments (purple) inside[184]. **d** | A DNA origami rotor enabling tracking the rotation of double-stranded DNA (dsDNA) relative to a genome-processing protein[223]. The dsDNA rotates when it is unwound by the protein bound on the substrate. The rotation can be amplified and tracked by the DNA origami rotor labelled with fluorescent dye (green star). **e** | A DNA origami force clamp[240]. Single-stranded DNA (ssDNA) exits the clamp duplexes in a shear conformation (left inset; scaffold in dark grey and staple in blue) and spans the 43-nm gap. ssDNA reservoirs are located on each side of the clamp. The system of interest (here, a DNA duplex) is probed in shear conformation (right inset; scaffold in dark grey and complementary DNA in pink). **f** | An icosahedral DNA origami nanoparticle (blue) presenting 10 copies of an HIV-1 envelope glycoprotein antigen (yellow) in a spatially organized manner[215]. **g** | A DNA origami ring (blue) carrying multiple lipidated handles (pink curl with blue head) as a template allowing formation of lipid vesicles (grey) with controlled size[253]. *F*, force. Part **b** adapted from REF.[195], Springer Nature Limited. Part **c** adapted with permission from REF.[184], AAAS. Part **d** adapted from REF.[223], Springer Nature Limited. Part **e** adapted with permission from REF.[240], AAAS. Part **f** adapted from REF.[215], Springer Nature Limited. Part **g** adapted from REF.[253], Springer Nature Limited.

Physiological and intracellular environments are highly heterogeneous and therefore call for smart carriers capable of sensing environmental stimuli at different delivery stages and switching their structures/properties to adapt to them. For example, Douglas et al. developed a logic-gated nanorobot (FIG. 6c) with a DNA origami container locked by two different aptamer motifs[184]. Only when both aptamers bind to the corresponding cell surface receptors can the container be opened (for example, an AND logic that gives a positive output only when all inputs are positive), which allows conditional exposure of the drug molecules to certain cell types. A later demonstration successfully cascaded multiple nanorobots into logic circuits, such as a half adder, in living cockroaches, enabling delivery of antibodies towards their cells based on calculation results[181]. In another example, a DNA origami nanorobot was constructed that could be selectively unfolded by nucleolin enriched in tumour-associated blood vessels. This allowed local exposure of the encapsulated thrombins and promoted intravascular thrombosis, resulting in tumour necrosis and inhibition of tumour growth in mice[40].

Compared with smaller DNA objects, such as tetrahedral DNA nanostructures that have also been intensively explored for drug delivery application[201,203], DNA origami structures yield more complex shapes spanning a wider range of dimensions (typically 2 nm to hundreds of nanometres). This enables higher loading capacity and more complex patterning of the drug payloads. Given that many biological effects such as ligand-receptor recognition[215] or cell internalization[209,210] are known to be sensitive in this dimension range, DNA origami may gain more traction for this application than smaller DNA objects.

Some issues remain, however, such as the stability of DNA origami structures in a biological environment[72] and possible immunogenicity of the exogenous nucleic acids[216]. Nevertheless, the potency of immunogenicity of these structures is highly dependent on the base sequence[217], structural properties[198] and chemical modifications[29,218]. Thus, by rationally engineering those parameters, the risk of immunotoxicity could be minimized[6,29,216–218]. By contrast, DNA structures with high immunogenicity can be used as adjuvants for vaccines in applications such as cancer immunotherapy[198,199].

Bioimaging and biophysics. DNA origami structures serve as standards, markers or structural support for molecules of interest in biophysical studies, allowing for the control and measurement of molecular stoichiometry, dimensions and collective behaviour. Placing a designated number of fluorophores at predefined positions on DNA origami structures (often sheets and rods) generates calibration standards or references for fluorescence microscopy to identify, count and measure the spacing between molecular species, for example fluorescently labelled protein constituents within a complex[34,106,219–222] (FIG. 3i). In some cases, a DNA origami structure helps to monitor biologically relevant movements just by virtue of their rigid body and well-defined shapes. For example, a DNA origami rotor was built with its centre attached to a dsDNA segment to track dsDNA rotations induced by the genome-processing enzymes RecBCD and RNA polymerase[223] (FIG. 6d). Similarly, stiff DNA rods enhance the signal to noise ratio of an optical trap[224,225] or FRET-based force measurement[226], leading to high-resolution study of weak biological forces (in the order of a few piconewtons) such as base stacking[225] and cell-substrate traction[226]. Labelling DNA filaments with motor proteins and fluorophores enables measurement of the velocity, processivity and stall force of myosin[115,227,228], dynein and kinesin[229], both individually and in motor ensembles.

In addition to optical imaging, DNA origami structures have been used to aid AFM and electron microscopy studies. 2D DNA origami sheets and frames are common substrates for AFM visualization of molecular motions[230] (FIG. 3g), including DNA structural transformations such as the B–Z transition[231] or the G-quadruplex formation[101], DNA–enzyme interactions such as transcription[232], recombination[233] and methylation[234], and movements of artificial DNA motors[108,177,235]. Clam-shaped DNA origami structures have facilitated the electron microscopy analyses of nucleosome interaction and stability, using their open or closed conformations to signify various states of nucleosome assembly[236–239]. A DNA origami 'force clamp' was built, where a U-shaped body suspends a segment of DNA under a defined tension of 0–12 pN (FIG. 6e) and enables single-molecule force spectroscopy studies of tension-dependent Holliday junction isomerization[240], DNA nuclease activities[241] and formation of the transcription pre-initiation complex[242]. Barrel or clamp-shaped 3D DNA origami structures have found applications in the cryo-EM structural determination of proteins, where DNA nanostructures serve to define the thickness of a vitrified ice sheet[243], create a hydrophobic environment to stabilize membrane proteins[244] and orient DNA-binding proteins at desired rotation angles[245].

DNA origami creates an artificial microenvironment to study the molecular mechanisms of biological processes. An illustrative example is the study of multivalent antigen–antibody and protein–aptamer bindings on a DNA origami platform, where antigens and aptamers are organized in assorted arrangements to identify the molecular patterns that contribute to avidity[215,246–248] (FIG. 6f). Crowding dsDNA with protospacer-adjacent motifs has led to enhanced Cas9/single guide RNA binding and more efficient dsDNA cleavage[249]. Varying the nucleoporin type and grafting density inside a DNA origami cylinder has been shown to significantly impact the collective morphology and conductance of the intrinsically disordered proteins[250,251]. Using DNA origami-templated liposome formation techniques (FIG. 6g), liposomes and membrane proteins have also been placed at defined distances and densities to study the biophysics of membrane dynamics[252–255]. Flat or curved DNA origami surfaces outfitted with amphipathic molecules such as cholesterol and peptides can lead to membrane binding and deformation and are useful for studying membrane mechanics[256–260]. Finally, DNA origami structures bridge the gap between top-down lithography-based devices, such as solid-state nanopores, and bottom-up molecular engineering, such as chemical synthesis and macromolecule self-assembly.

Avidity
The molecular binding strength as a result of multiple, non-covalent interactions, for example between an antibody and a complex antigen.

They can therefore create advanced analytical tools, for example signal-enhanced long-distance FRET pairs[261] or nanopores for measuring molecular recognition[262,263], for biophysical experiments.

Reproducibility and data deposition

The general standards of DNA origami assembly have been continuously developed, ranging from DNA origami designs to purification methods to reconstruction models for TEM imaging, among others[73,264]. To ensure high reproducibility, several important aspects should be carefully examined.

First, although a one-pot reaction can be used for the self-assembly of DNA origami, this often results in many by-products such as dimers, trimers and other aggregates. Various assembly conditions, such as the annealing procedure and the cationic strength, can significantly influence the yields of the target products and by-products. Optimization of the annealing procedure, especially the annealing temperature intervals, is crucial to achieving the target object with high yield. Furthermore, cationic strength is another critical parameter for optimization in order to avoid DNA origami dissociation through electrostatic repulsion. The TAE buffer with Mg^{2+} (5–20 mM) is typically adopted in most protocols for DNA origami assembly.

Second, purification of the DNA origami is of great importance. There are five typical purification methods: PEG precipitation, gel purification, filter purification, ultracentrifugation and size-exclusion chromatography. The most appropriate purification method for a particular experiment should be selected based on the yield and duration as well as the volume limitation, dilution, residuals and damage[46,73] For example, PEG precipitation can be adapted to enhance the recovery yield of target species after purification, but it also introduces residual PEG molecules. Filter purification with molecular weight cut-off membranes provides residual-free separation. Although it has volume limitations, this is an effective method to quickly separate DNA origami from excess strands (≈30 min) and to adjust buffer conditions. Gel purification is suitable for bandpass molecular weight separation, such as complex DNA origami structures and nanoparticles. Size-exclusion chromatography is suitable for bandpass molecular weight separation without introducing residual compounds and is commonly employed in protein biochemistry.

Last, the storage temperature and the cationic strength are both crucial for DNA origami stabilization. In general, DNA origami is thermally stable at temperatures ≤55 °C in solution. However, it can also be stable at temperatures >85 °C with photo-cross-linking-assisted thermal stability[80]. DNA origami can also be lyophilized and stored under freezing conditions[265]. For the cationic strength, many approaches have been reported to protect DNA origami from destabilization, especially at low Mg^{2+} concentrations or without Mg^{2+} (REFS[70,71]). In addition, block copolymers could be a reversible protection and potential long-term storage strategy for DNA origami nanostructures as they can protect nanostructures from low-salt denaturation and nuclease degradation[30,266].

To ensure data reproducibility, researchers must provide sufficient general information as well as detailed experimental conditions and procedures in their publications. For instance, general information including DNA origami design, assembly and purification procedures, quality analysis approaches, AFM and TEM sample preparations and data pre-processing should be provided. For hybrid DNA origami structures, modifications of the attached nanoparticles or proteins, their conjugations on the DNA origami and the purification procedures of such DNA origami complexes should be carefully described. For drug delivery using DNA origami, it is often difficult to unify the minimum reporting standards owing to the complexity of biological experiments. Typically, this method can follow the general rules required by biological journals. In addition, the experimental protocols and methods, assembly materials and sources, design and analysis software should also be carefully listed and described in detail. Free software, such as CaDNAno and EMAN2, may be deposited in an open source repository. Finally, data deposition in public repositories is highly recommended. For example, scaffold sequences can be deposited in GenBank.

Limitations and optimizations

The remarkable breadth of applications not only highlights the power of DNA origami but also reveals roadblocks that need to be removed in order for the technology to reach its full potential. Somewhat surprisingly, the first limitation is the structural design of DNA origami, which, to date, remains a hurdle for those new to DNA nanotechnology and is sometimes challenging even for users familiar with the technique. Although many design and simulation tools[8–10,15,47–50,56,59,61–63,73,267–274] have been developed and made available to the public, the more versatile design tools generally require a considerable amount of user input and technical know-how. In addition, the better automated tools are typically geared towards specific types of construct, such as 2D meshes with a triangulated framework[48] or wireframe polyhedrons[9,15,47]. Ideally, we would enjoy a suite of software that streamline the design and simulation process, serving both as a tool to easily convert simple geometrical models into DNA origami designs and as a sandbox for users to explore new design concepts. The field has made steady strides towards this goal by interfacing multiple design-simulation software, developing more user-friendly interfaces and allowing for post-simulation touch-up to optimize design iteratively.

Second, the functionalization of DNA nanostructures in most cases necessitates chemically modifying DNA with molecules of interest. Even with a multitude of well-documented DNA-modification chemistries and a continuous stream of emerging bioconjugation methods, finding a robust and controllable conjugation method for a specific application can be a daunting task. A few review articles[116,275,276] summarize the field's progress in this area. Although the most appropriate conjugation method depends on the application, good candidates are generally easy to perform in that they require few steps and use commonly available chemicals, generate stable products with decent yield, allow stoichiometric

control and retain the structure and function of the DNA-modifying moieties. Of equal importance to selecting a suitable conjugation chemistry are careful optimization and rigorous quality control when placing guest molecules on DNA origami structures. These include purifying functionalized DNA structures[84], quantifying the labelling efficiency and examining/eradicating any undesired behaviours, such as aggregation or loss of fluorescence, as a result of DNA attachment.

Third, a clear picture of the DNA origami assembly mechanism remains elusive. Although we are equipped with advanced techniques to design and produce desired DNA origami shapes, we need to better understand how hundreds of DNA strands self-assemble to form such complex structures. Besides driving a higher assembly yield of the target structures, the ability to clearly define DNA origami folding pathways will enable rationally designed dynamic assemblies that can toggle between a few metastable conformations with low energy barriers between them, which is a feature found in many protein machineries. Numerous high-quality studies have shed light on this long-standing question, including systematically testing DNA origami design variants that lead to different folding outcomes[11,69,277], measuring the global thermal transition during DNA origami assembly and disassembly[76], directly observing assembly intermediates[98] and monitoring the incorporation of selected staple strands[12,92]. Many of these studies suggest a multistage, cooperative folding behaviour. Future efforts to depict such complex mechanisms will benefit from high-throughput analytical methods[278] and simulation frameworks[50,56,59,61–63,73,270,271] for DNA self-assembly.

Fourth, the size of a DNA origami structure is limited by the length of its scaffold strand, typically 7–8 kb long. To obtain larger structures, one has to use a longer scaffold[65,67] and/or stitch multiple DNA origami structures together[20,21,26,279]. Both methods have been successful thanks to bacteriophage genome engineering and hierarchical DNA self-assembly[81,280–282] via sticky-end cohesion or blunt-end base stacking. These successes, however, often come at the expense of a marginal to severe drop in assembly yield. Although the field has largely relied on the M13 phage genome as scaffold strands for DNA origami production, ssDNAs that are multi-kilobases long with fully customizable sequences are now available[68,217]. Thus, in principle, a geometrically complex, fully addressable DNA origami structure can be synthesized from multiple scaffolds of orthogonal sequences in one pot, circumventing certain problems associated with exceedingly long ssDNA, such as instability or kinetic traps, and hierarchical self-assembly, such as slowness and reduced efficiency. A related practical issue is how to generate staple strands in a cost-effective way to fold these massive structures (that can reach the gigadalton scale) in large quantities. The most promising solutions today are enzyme-mediated in vitro amplification of synthetic DNA oligonucleotides[283,284] and biological production of DNA strands in bacteriophages[283,285]. Using the latter approach, several hundred milligrams of DNA origami structures were produced at a fraction of the cost of using conventional synthetic DNA[285].

Last, certain intrinsic properties of DNA, such as its negative charge and susceptibility to enzyme degradation, may limit its applications, especially in a biological environment (for example, to deliver drugs to the bloodstream or the intracellular space)[29]. On the other hand, certain applications in physics and materials science, such as high-temperature etching or 3D lithography, can test the thermal and mechanical stability of DNA origami structures. In this case, the physical performance of DNA origami can be enhanced with a combination of DNA modification chemistries such as photo-cross-linking DNA nucleotides[80,286,287], wrapping exposed DNA surfaces with lipid bilayers[29], shielding DNA backbones with polycationic polymers[30,218,266,288–290] and coating DNA with silica[28]. By chemically or physically separating DNA from the environment and strengthening the links between DNA strands, these modifications help DNA origami structures survive low-salt, high-heat conditions, resist nuclease digestion, evade immune surveillance, prolong in vivo circulation and avoid surface deformation.

Outlook

The future of the DNA origami technique, and structural DNA nanotechnology more generally, will be shaped by ambitious technology developers constantly pushing technological frontiers and a diverse group of users, who will introduce new inspirations and challenges to fuel future innovations. Interesting scientific questions that will have to be addressed involve improvement of the chemical versatility of the structures, further improving speed and robustness of folding, and the realization of isothermal and in vivo assembly of nucleic acid nanostructures. Improved chemical versatility will enable novel applications in materials science, catalysis, nanomedicine and molecular robotics, whereas isothermal and in vivo assembly will be important for biomedical applications and synthetic biology.

Molecular programming and automation. DNA origami is a robust, sequence-programmable, nanometre-precise self-assembly technique, which is amenable to automation. It is not incidental that researchers in DNA nanotechnology and computing have dubbed their approach molecular programming. Quite literally, DNA origami structures can be programmed using computer-aided tools[8,15] without much knowledge about their chemical details. Arguably, the development of the caDNAno design program was one of the major catalysts for the field[8], allowing even newcomers to design complicated supramolecular structures with a good chance of success. Since then, a series of other design software packages have been developed for different types of origami structure (TABLE 1).

It is therefore expected that one line of research will continue to be devoted to the molecular programming of nanostructures. This will involve an even stronger interconnection between computational design, automated synthesis and assembly of the structures. This could ultimately lead to a completely automated process for the generation of DNA-based nanostructures potentially combined with on-demand DNA synthesis[291] (FIG. 7A).

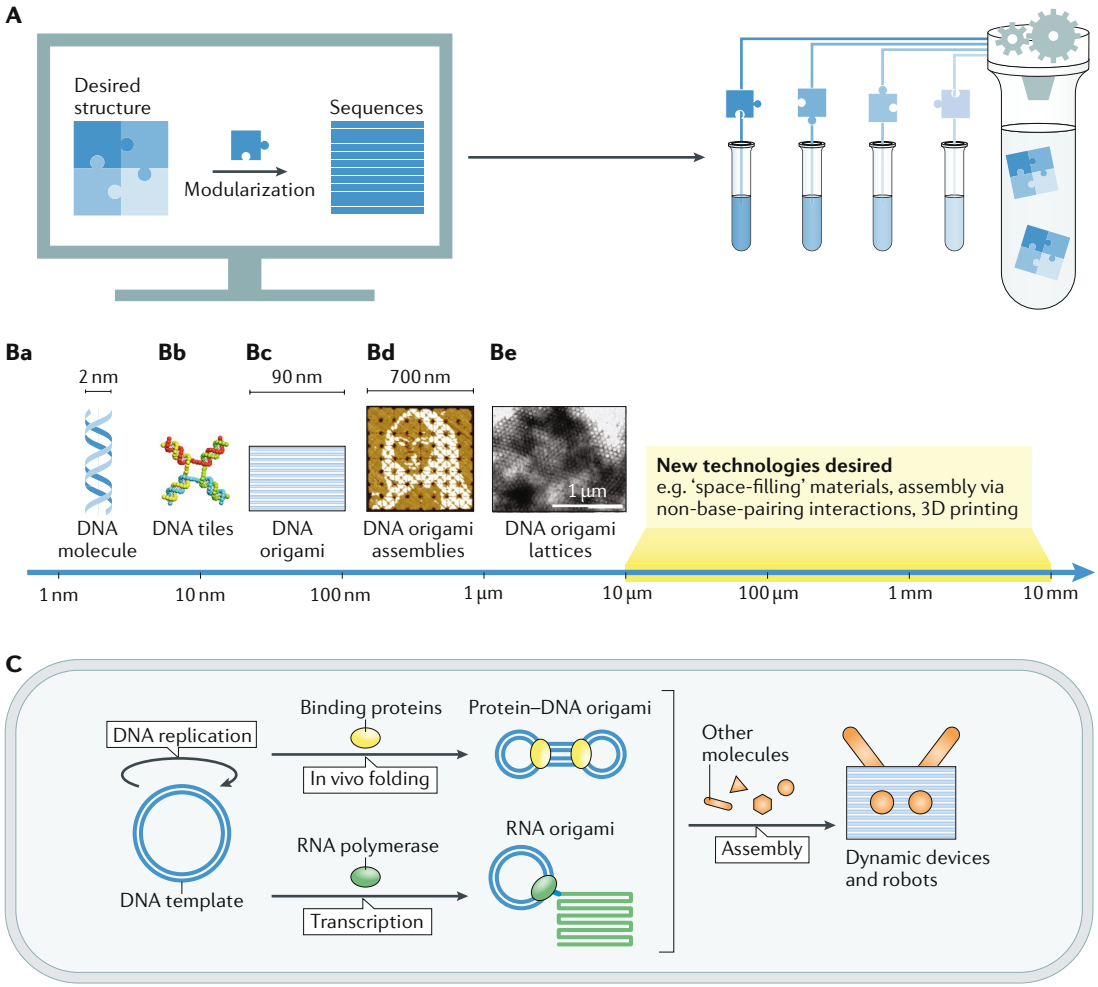

Fig. 7 | **Outlook for DNA origami technology. A** | Modular, computer-aided design and automated fabrication. We expect that the integration of these techniques could lead to a completely automated process for the generation of on-demand nanostructures, without the need for much knowledge about their chemical details. **B** | Multiscale manufacturing will require the integration of different, scale-dependent assembly strategies into a consistent workflow — ranging from the formation of DNA helices (part **a**) over DNA tiles[74] (part **b**) to origami structures[7] (part **c**) and larger assemblies, such as DNA origami arrays[21] (part **d**) and 3D crystals[82] (part **e**). Even larger length scales may be accessed by interfacing origami with other (non-DNA) manufacturing technologies[21,74,82]. **C** | In vivo production of DNA/RNA origami and further assembly of dynamic devices and robots. DNA templates (blue) may be replicated in vivo and folded with intracellular DNA-binding proteins (yellow), forming protein–DNA origami structures[303]; or they can be transcribed into RNA origami structures when transcribed by RNA polymerase (green)[23,299,304]. These nucleic acid structures can be further integrated with other intracellular components (orange) to form dynamic devices and robots in vivo. Part **Bb** adapted with permission from REF.[74], ACS. Part **Bc** adapted from REF.[7], Springer Nature Limited. Part **Bd** adapted from REF.[21], Springer Nature Limited. Part **Be** adapted with permission from REF.[82], Wiley.

Design rules are expected to further improve based on a better biophysical understanding of the origami folding process.

Chemistry for applications. DNA origami has become popular because it meets the need for a molecular technology that enables the positioning of molecules and nanoparticles with nanometre precision and with a defined stoichiometry, potentially addressing a wide range of problems in nanoscience and in the life sciences.

As the origami field moves more towards applications, most researchers will deal less with the refinement of the technique itself than with coping with the specifics of their application. Much future research will therefore be devoted to resolving chemical requirements specific to certain applications, such as making DNA origami chemically and physically stable, and developing molecular adaptors for functional components[116]. Chemical stability will involve modified DNA and the careful design of sequence and structure to avoid undesired binding and degradation or disruption by enzymes. Physical stability — by which we mean both thermal and mechanical — can be enhanced by cross-linking or addition of stabilizing ions and surfactants. In addition, a better mechanistic understanding of the origami assembly/disassembly process will also clarify which types of origami design provide the highest physical stability.

Tectons
Structural motifs that serve as units for assembly of higher order structures.

Xeno-nucleic acids
(XNAs). Artificially synthesized nucleic acids that do not exist in nature (for example, nucleic acids carrying unnatural backbones, bases or chemical modifications).

Dynamic devices and robots. One of the frontiers of DNA nanotechnology is the use of origami structures as components for molecular robots. The complexity of origami structures allows the integration of multiple functions in one device, which is required for molecular robots that involve the interplay of sensing, computing and actuation modalities within a molecular system. One of the most promising applications for such systems will be in the context of biomedical nanorobotics, which will continue to be an intensive field of research over the next decade[184].

As parts of molecular assembly lines, origami-based nanorobots could perform mechanical synthesis of molecules by bringing components into proximity and appropriate orientation for a reaction[292,293] based on instructions read from a molecular tape. It is conceivable that catalytic origami structures could be developed that promote the reaction between two or more molecular components localized to the structures. Potentially, these reactions could be coupled to conformational changes of the origami structures, which could be either driven by some energy-consuming chemical process or physically driven using external fields[110,116,294].

Multiscale molecular manufacturing. Even though origami structures provide a means to control matter at the 10–100 nm length scale, it is unlikely that the technique will be applied to the creation of much larger structures. Instead, future research will be devoted to developing strategies for multiscale integration of DNA origami objects. This will involve combination with 'space-filling' materials other than DNA, and self-assembly or printing of origami tectons into discrete or crystalline higher order structures using interactions other than DNA base pairing[20] (FIG. 7).

DNA origami will continue to be used to explore fundamental questions of self-assembly and self-organization, which may give rise to completely novel assembly strategies. Although nature uses many non-equilibrium self-assembly processes, their use in the context of DNA nanostructures is still largely underexplored. Coupling DNA self-assembly to energy-consuming processes will open up new possibilities for dynamically assembling[295] active molecular materials. One of the great visions in this context is the creation of molecular systems capable of self-replication[296].

Generalizing the origami idea. The existing origami technique still has several shortcomings: for instance, DNA structures defined on lattices only have a limited spatial resolution essentially defined by the interhelix distance (≈2–3 nm). Another issue is the restricted chemical functionality of DNA, usually necessitating chemical modification of DNA staple strands. Finally, for some applications it may be desirable to produce origami-like structures inside living cells.

The origami idea is based on the use of scaffold structures and proximity effects to enhance sequence-encoded molecular self-assembly. The resulting robust assembly processes are amenable to abstraction and high-level molecular programming and can therefore be easily adopted by non-experts. Future efforts will be devoted to the question of whether this idea can be extended in scope, applied to other molecules and made to work in vivo. Several groups have already started to create lattice-free origami structures[47] that allow folding of structures in wireframes or along arbitrary object-filling curves. In order to increase chemical versatility, it will be interesting to explore whether the same underlying principles that enable DNA origami can contribute to the design of protein nanostructures. Hybrid approaches are conceivable, in which DNA or RNA scaffolds support the association of proteins into heteromultimeric complexes. An exciting alternative is the extension of the chemical capabilities of origami using xeno-nucleic acids (XNAs) with different backbones and unnatural base pairs[297,298].

In vivo production. Although the production of origami scaffolds and staples inside cells has been successfully demonstrated[285], it is hard to imagine that the annealing of hundreds of oligonucleotides would work in this context. Instead, intramolecular folding of structures appears to be more promising and there has been great progress in the development of ssDNA origami[23] and RNA origami[299]. RNA nanostructures can be produced co-transcriptionally, for example folded while the constituting RNA strand is generated by an RNA polymerase. In contrast to DNA origami, this type of folding is an isothermal process, the outcome of which is influenced by the competition of intramolecular folding kinetics and the speed of transcription. Clever design of such processes — including the presence of RNA-binding proteins — could result in ribonucleoprotein nanostructures that, similar to ribosomes, are quite stable in a cellular environment.

Single-stranded RNA or DNA origami can be produced by template-directed enzymatic synthesis. As XNAs are designed to be compatible with biopolymerization processes, they could also be included in enzymatically produced nanostructures. An exciting perspective could thus be an expansion of the genetic alphabet to code for XNA-based nanostructures that can be synthesized in vivo. First experiments have shown that bacteria containing unnatural base pairs can replicate, and thus bacterial strains could be developed that act as XNA origami producers[300]. Coupling the production of DNA, RNA or XNA origami to reproduction opens up the possibility of evolutionary optimization, which could result in even more complex structures with completely novel functionalities.

Published online: 28 January 2021

1. Seeman, N. C. Nucleic-acid junctions and lattices. *J. Theor. Biol.* **99**, 237–247 (1982).
This study, as the beginning of DNA nanotechnology, theoretically predicts immobile branched DNA junctions and their 3D assemblies.
2. Fu, T. J. & Seeman, N. C. DNA double-crossover molecules. *Biochemistry* **32**, 3211–3220 (1993).
3. LaBean, T. H. et al. Construction, analysis, ligation, and self-assembly of DNA triple crossover complexes. *J. Am. Chem. Soc.* **122**, 1848–1860 (2000).
4. Yan, H., Park, S. H., Finkelstein, G., Reif, J. H. & LaBean, T. H. DNA-templated self-assembly of protein arrays and highly conductive nanowires. *Science* **301**, 1882–1884 (2003).
5. He, Y. et al. Hierarchical self-assembly of DNA into symmetric supramolecular polyhedra. *Nature* **452**, 198–201 (2008).
6. Seeman, N. C. & Sleiman, H. F. DNA nanotechnology. *Nat. Rev. Mater.* **3**, 17068 (2017).
This review provides a more comprehensive view of DNA nanotechnology, covering branches other than DNA origami.

7. Rothemund, P. W. K. Folding DNA to create nanoscale shapes and patterns. *Nature* **440**, 297–302 (2006). **This study is the first demonstration of DNA origami**.
8. Douglas, S. M. et al. Rapid prototyping of 3D DNA origami shapes with caDNAno. *Nucleic Acids Res.* **37**, 5001–5006 (2009). **This study provides a 1G visual DNA origami design tool that is an important catalyst for this field**.
9. Jun, H. et al. Automated sequence design of 3D polyhedral wireframe DNA origami with honeycomb edges. *ACS Nano* **13**, 2083–2093 (2019).
10. Jun, H., Wang, X., Bricker, W. P. & Bathe, M. Automated sequence design of 2D wireframe DNA origami with honeycomb edges. *Nat. Commun.* **10**, 5419 (2019).
11. Dunn, K. E. et al. Guiding the folding pathway of DNA origami. *Nature* **525**, 82–86 (2015). **This study explains why DNA origami can generate desired shapes with high yields, from the perspective of cooperativity in folding**.
12. Schneider, F., Möritz, N. & Dietz, H. The sequence of events during folding of a DNA origami. *Sci. Adv.* **5**, eaaw1412 (2019).
13. Qian, L. et al. Analogic China map constructed by DNA. *Chin. Sci. Bull.* **51**, 2973 (2006).
14. Andersen, E. S. et al. DNA origami design of dolphin-shaped structures with flexible tails. *ACS Nano* **2**, 1213–1218 (2008).
15. Benson, E. et al. DNA rendering of polyhedral meshes at the nanoscale. *Nature* **523**, 441–444 (2015). **This paper presents a general and automated design method based on graph theory for building arbitrary polygonal structures that are difficult to realize using previous approaches**.
16. Sun, W. et al. Casting inorganic structures with DNA molds. *Science* **346**, 1258361 (2014).
17. Douglas, S. M. et al. Self-assembly of DNA into nanoscale three-dimensional shapes. *Nature* **459**, 414–418 (2009). **This study demonstrates the building of 3D DNA origami structures in form of honeycomb lattices**.
18. Dietz, H., Douglas, S. M. & Shih, W. M. Folding DNA into twisted and curved nanoscale shapes. *Science* **325**, 725–730 (2009). **This study demonstrates the construction of DNA origami shapes with quantitative twists and curvatures, by rational insertions and deletions of base pairs into and from the DNA bundles**.
19. Han, D. et al. DNA origami with complex curvatures in three-dimensional space. *Science* **332**, 342–346 (2011).
20. Wagenbauer, K. F., Sigl, C. & Dietz, H. Gigadalton-scale shape-programmable DNA assemblies. *Nature* **552**, 78–83 (2017).
21. Tikhomirov, G., Petersen, P. & Qian, L. Fractal assembly of micrometre-scale DNA origami arrays with arbitrary patterns. *Nature* **552**, 67–71 (2017).
22. Yao, G. et al. Meta-DNA structures. *Nat. Chem.* **12**, 1067–1075 (2020).
23. Han, D. et al. Single-stranded DNA and RNA origami. *Science* **358**, eaao2648 (2017).
24. Geary, C., Rothemund, P. W. K. & Andersen, E. S. A single-stranded architecture for cotranscriptional folding of RNA nanostructures. *Science* **345**, 799–804 (2014). **This study demonstrates the potential of synthesizing origami-like RNA nanostructures in biological systems**.
25. Zhang, D. Y. & Seelig, G. Dynamic DNA nanotechnology using strand-displacement reactions. *Nat. Chem.* **3**, 103–113 (2011).
26. Gerling, T., Wagenbauer, K. F., Neuner, A. M. & Dietz, H. Dynamic DNA devices and assemblies formed by shape-complementary, non-base pairing 3D components. *Science* **347**, 1446–1452 (2015). **This study demonstrates that DNA origami structures can be further assembled into higher order yet dynamically reconfigurable structures based on shape complementarity rather than base pairing, which provides an approach to overcome the size limit of DNA origami**.
27. Ge, Z., Gu, H., Li, Q. & Fan, C. Concept and development of framework nucleic acids. *J. Am. Chem. Soc.* **140**, 17808–17819 (2018).
28. Liu, X. et al. Complex silica composite nanomaterials templated with DNA origami. *Nature* **559**, 593–598 (2018).
29. Perrault, S. D. & Shih, W. M. Virus-inspired membrane encapsulation of DNA nanostructures to achieve in vivo stability. *ACS Nano* **8**, 5132–5140 (2014).
30. Agarwal, N. P., Matthies, M., Gur, F. N., Osada, K. & Schmidt, T. L. Block copolymer micellization as a protection strategy for DNA origami. *Angew. Chem. Int. Ed.* **56**, 5460–5464 (2017).
31. Liu, N. & Liedl, T. DNA-assembled advanced plasmonic architectures. *Chem. Rev.* **118**, 3032–3053 (2018). **This review focuses on the progress of using DNA nanostructures as scaffolds for creating plasmonic architectures, which is an important field for nanophotonic applications**.
32. Maune, H. T. et al. Self-assembly of carbon nanotubes into two-dimensional geometries using DNA origami templates. *Nat. Nanotechnol.* **5**, 61–66 (2010).
33. Jin, Z. et al. Metallized DNA nanolithography for encoding and transferring spatial information for graphene patterning. *Nat. Commun.* **4**, 1663 (2013).
34. Jungmann, R. et al. Multiplexed 3D cellular super-resolution imaging with DNA-PAINT and Exchange-PAINT. *Nat. Methods* **11**, 313–318 (2014).
35. Nicoli, F. et al. Directional photonic wire mediated by homo-Förster resonance energy transfer on a DNA origami platform. *ACS Nano* **11**, 11264–11272 (2017).
36. Dutta, P. K. et al. DNA-directed artificial light-harvesting antenna. *J. Am. Chem. Soc.* **133**, 11985–11993 (2011).
37. Yurke, B., Turberfield, A. J., Mills, A. P., Simmel, F. C. & Neumann, J. L. A DNA-fuelled molecular machine made of DNA. *Nature* **406**, 605–608 (2000).
38. Lu, C. H. & Willner, I. Stimuli-responsive DNA-functionalized nano-/microcontainers for switchable and controlled release. *Angew. Chem. Int. Ed.* **54**, 12212–12235 (2015).
39. Jiang, Q., Liu, S., Liu, J., Wang, Z. & Ding, B. Rationally designed DNA origami nanomaterials for drug delivery in vivo. *Adv. Mater.* **31**, e1804785 (2019). **This review focuses on the progress in drug delivery application based on DNA origami**.
40. Li, S. et al. A DNA nanorobot functions as a cancer therapeutic in response to a molecular trigger in vivo. *Nat. Biotechnol.* **36**, 258–264 (2018).
41. Li, J., Green, A. A., Yan, H. & Fan, C. Engineering nucleic acid structures for programmable molecular circuitry and intracellular biocomputation. *Nat. Chem.* **9**, 1056–1067 (2017).
42. Thubagere, A. J. et al. A cargo-sorting DNA robot. *Science* **357**, eaan6558 (2017).
43. Chao, J. et al. Solving mazes with single-molecule DNA navigators. *Nat. Mater.* **18**, 273–279 (2019).
44. Kuzyk, A. et al. A light-driven three-dimensional plasmonic nanosystem that translates molecular motion into reversible chiroptical function. *Nat. Commun.* **7**, 10591 (2016).
45. Zhang, F. et al. Complex wireframe DNA origami nanostructures with multi-arm junction vertices. *Nat. Nanotechnol.* **10**, 779–784 (2015).
46. Wagenbauer, K. F. et al. How we make DNA origami. *ChemBioChem* **18**, 1873–1885 (2017).
47. Veneziano, R. et al. Designer nanoscale DNA assemblies programmed from the top down. *Science* **352**, 1534 (2016).
48. Benson, E. et al. Computer-aided production of scaffolded DNA nanostructures from flat sheet meshes. *Angew. Chem. Int. Ed.* **55**, 8869–8872 (2016).
49. Jun, H. et al. Autonomously designed free-form 2D DNA origami. *Sci. Adv.* **5**, eaav0655 (2019).
50. Huang, C.-M., Kucinic, A., Johnson, J. A., Su, H.-J. & Castro, C. E. Integrating computer-aided engineering and computer-aided design for DNA assemblies. Preprint at *bioRxiv* https://doi.org/10.1101/2020.05.28.119701 (2020).
51. Jun, H., Wang, X., Bricker, W. P., Jackson, S. & Bathe, M. Rapid prototyping of wireframe scaffolded DNA origami using ATHENA. Preprint at *bioRxiv* https://doi.org/10.1101/2020.02.09.940320 (2020).
52. de Llano, E. et al. Adenita: interactive 3D modelling and visualization of DNA nanostructures. *Nucleic Acids Res.* **48**, 8269–8275 (2020).
53. Yoo, J. & Aksimentiev, A. In situ structure and dynamics of DNA origami determined through molecular dynamics simulations. *Proc. Natl Acad. Sci. USA* **110**, 20099–20104 (2013).
54. Göpfrich, K. et al. Large-conductance transmembrane porin made from DNA origami. *ACS Nano* **10**, 8207–8214 (2016).
55. Savelyev, A. & Papoian, G. A. Molecular renormalization group coarse-graining of polymer chains: application to double-stranded DNA. *Biophys. J.* **96**, 4044–4052 (2009).
56. Pan, K. et al. Lattice-free prediction of three-dimensional structure of programmed DNA assemblies. *Nat. Commun.* **5**, 5578 (2014).
57. Nakano, S. Nucleic acid duplex stability: influence of base composition on cation effects. *Nucleic Acids Res.* **27**, 2957–2965 (1999).
58. Wohlert, J., den Otter, W. K., Edholm, O. & Briels, W. J. Free energy of a trans-membrane pore calculated from atomistic molecular dynamics simulations. *J. Chem. Phys.* **124**, 154905 (2006).
59. Reshetnikov, R. V. et al. A coarse-grained model for DNA origami. *Nucleic Acids Res.* **46**, 1102–1112 (2018).
60. Poppleton, E. et al. Design, optimization and analysis of large DNA and RNA nanostructures through interactive visualization, editing and molecular simulation. *Nucleic Acids Res.* **48**, e72 (2020).
61. Doye, J. P. K. et al. Coarse-graining DNA for simulations of DNA nanotechnology. *Phys. Chem. Chem. Phys.* **15**, 20395–20414 (2013).
62. Snodin, B. E. K. et al. Introducing improved structural properties and salt dependence into a coarse-grained model of DNA. *J. Chem. Phys.* **142**, 234901 (2015).
63. Maffeo, C. & Aksimentiev, A. MrDNA: a multi-resolution model for predicting the structure and dynamics of DNA systems. *Nucleic Acids Res.* **48**, 5135–5146 (2020).
64. Veneziano, R. et al. In vitro synthesis of gene-length single-stranded DNA. *Sci. Rep.* **8**, 6548 (2018).
65. Zhang, H. et al. Folding super-sized DNA origami with scaffold strands from long-range PCR. *Chem. Commun.* **48**, 6405–6407 (2012).
66. Erkelenz, M. et al. A facile method for preparation of tailored scaffolds for DNA origami. *Small* **10**, 73–77 (2014).
67. Marchi, A. N., Saaem, I., Vogen, B. N., Brown, S. & LaBean, T. H. Toward larger DNA origami. *Nano Lett.* **14**, 5740–5747 (2014).
68. Nafisi, P. M., Aksel, T. & Douglas, S. M. Construction of a novel phagemid to produce custom DNA origami scaffolds. *Synth. Biol.* **3**, ysy015 (2018).
69. Ke, Y., Bellot, G., Voigt, N. V., Fradkov, E. & Shih, W. M. Two design strategies for enhancement of multilayer-DNA origami folding: underwinding for specific intercalator rescue and staple-break positioning. *Chem. Sci.* **3**, 2587–2597 (2012).
70. Martin, T. G. & Dietz, H. Magnesium-free self-assembly of multi-layer DNA objects. *Nat. Commun.* **3**, 1103 (2012).
71. Kielar, C. et al. On the stability of DNA origami nanostructures in low-magnesium buffers. *Angew. Chem. Int. Ed.* **57**, 9470–9474 (2018).
72. Hahn, J., Wickham, S. F., Shih, W. M. & Perrault, S. D. Addressing the instability of DNA nanostructures in tissue culture. *ACS Nano* **8**, 8765–8775 (2014).
73. Castro, C. E. et al. A primer to scaffolded DNA origami. *Nat. Methods* **8**, 221–229 (2011).
74. Hong, F., Zhang, F., Liu, Y. & Yan, H. DNA origami: scaffolds for creating higher order structures. *Chem. Rev.* **117**, 12584–12640 (2017).
75. Schickinger, M., Zacharias, M. & Dietz, H. Tethered multifluorophore motion reveals equilibrium transition kinetics of single DNA double helices. *Proc. Natl Acad. Sci. USA* **115**, E7512–E7521 (2018).
76. Sobczak, J.-P. J., Martin, T. G., Gerling, T. & Dietz, H. Rapid folding of DNA into nanoscale shapes at constant temperature. *Science* **338**, 1458–1461 (2012).
77. Liu, W., Zhong, H., Wang, R. & Seeman, N. C. Crystalline two-dimensional DNA origami arrays. *Angew. Chem. Int. Ed.* **50**, 264–267 (2011).
78. Kocabey, S. et al. Membrane-assisted growth of DNA origami nanostructure arrays. *ACS Nano* **9**, 3530–3539 (2015).
79. Suzuki, Y., Endo, M. & Sugiyama, H. Lipid-bilayer-assisted two-dimensional self-assembly of DNA origami nanostructures. *Nat. Commun.* **6**, 1–9 (2015).
80. Rajendran, A., Endo, M., Katsuda, Y., Hidaka, K. & Sugiyama, H. Photo-cross-linking-assisted thermal stability of DNA origami structures and its application for higher-temperature self-assembly. *J. Am. Chem. Soc.* **133**, 14488–14491 (2011).
81. Woo, S. & Rothemund, P. W. K. Programmable molecular recognition based on the geometry of DNA nanostructures. *Nat. Chem.* **3**, 620–627 (2011).
82. Zhang, T. et al. 3D DNA origami crystals. *Adv. Mater.* **30**, 1800273 (2018).
83. Bellot, G., McClintock, M. A., Lin, C. & Shih, W. M. Recovery of intact DNA nanostructures after agarose gel-based separation. *Nat. Methods* **8**, 192–194 (2011).
84. Shaw, A., Benson, E. & Högberg, B. Purification of functionalized DNA origami nanostructures. *ACS Nano* **9**, 4968–4975 (2015).

85. Stahl, E., Martin, T. G., Praetorius, F. & Dietz, H. Facile and scalable preparation of pure and dense DNA origami solutions. *Angew. Chem. Int. Ed.* **53**, 12735–12740 (2014).
86. Lin, C., Perrault, S. D., Kwak, M., Graf, F. & Shih, W. M. Purification of DNA origami nanostructures by rate-zonal centrifugation. *Nucleic Acids Res.* **41**, e40–e40 (2013).
87. Wagenbauer, K. F., Wachauf, C. H. & Dietz, H. Quantifying quality in DNA self-assembly. *Nat. Commun.* **5**, 3691 (2014).
88. Sacca, B. et al. Reversible reconfiguration of DNA origami nanochambers monitored by single-molecule FRET. *Angew. Chem. Int. Ed.* **54**, 3592–3597 (2015).
89. Andersen, E. S. et al. Self-assembly of a nanoscale DNA box with a controllable lid. *Nature* **459**, 73–76 (2009).
This work presents a DNA origami container whose lid can be dynamically opened via toehold-mediated strand displacement, which inspires later studies on controllable cargo release.
90. Grossi, G., Jepsen, M. D. E., Kjems, J. & Andersen, E. S. Control of enzyme reactions by a reconfigurable DNA nanovault. *Nat. Commun.* **8**, 992 (2017).
91. Wei, X., Nangreave, J. & Liu, Y. Uncovering the self-assembly of DNA nanostructures by thermodynamics and kinetics. *Acc. Chem. Res.* **47**, 1861–1870 (2014).
92. Wei, X., Nangreave, J., Jiang, S., Yan, H. & Liu, Y. Mapping the thermal behavior of DNA origami nanostructures. *J. Am. Chem. Soc.* **135**, 6165–6176 (2013).
93. Opherden, L., Oertel, J., Barkleit, A., Fahmy, K. & Keller, A. Paramagnetic decoration of DNA origami nanostructures by Eu^{3+} coordination. *Langmuir* **30**, 8152–6159 (2014).
94. Schreiber, R. et al. Chiral plasmonic DNA nanostructures with switchable circular dichroism. *Nat. Commun.* **4**, 2948 (2013).
95. Rajendran, A., Endo, M. & Sugiyama, H. Single-molecule analysis using DNA origami. *Angew. Chem. Int. Ed.* **51**, 874–890 (2012).
96. Birkedal, V. et al. Single molecule microscopy methods for the study of DNA origami structures. *Microsc. Res. Tech.* **74**, 688–698 (2011).
97. Jungmann, R., Scheible, M. & Simmel, F. C. Nanoscale imaging in DNA nanotechnology. *Wiley Interdiscip. Rev. Nanomed. Nanobiotechnol.* **4**, 66–81 (2012).
98. Wah, J. L., David, C., Rudiuk, S., Baigl, D. & Estevez-Torres, A. Observing and controlling the folding pathway of DNA origami at the nanoscale. *ACS Nano* **10**, 1978–1987 (2016).
99. Kosinski, R. et al. Sites of high local frustration in DNA origami. *Nat. Commun.* **10**, 1061 (2019).
100. Song, J. et al. Reconfiguration of DNA molecular arrays driven by information relay. *Science* **357**, eaan3377 (2017).
101. Sannohe, Y., Endo, M., Katsuda, Y., Hidaka, K. & Sugiyama, H. Visualization of dynamic conformational switching of the G-quadruplex in a DNA nanostructure. *J. Am. Chem. Soc.* **132**, 16311–16313 (2010).
102. Endo, M., Katsuda, Y., Hidaka, K. & Sugiyama, H. A versatile DNA nanochip for direct analysis of DNA base-excision repair. *Angew. Chem. Int. Ed.* **49**, 9412–9416 (2010).
103. Ramakrishnan, S. et al. Real-time observation of superstructure-dependent DNA origami digestion by DNase I using high-speed atomic force microscopy. *ChemBioChem* **20**, 2818–2823 (2019).
104. Bai, X. C., Martin, T. G., Scheres, S. H. & Dietz, H. Cryo-EM structure of a 3D DNA origami object. *Proc. Natl Acad. Sci. USA* **109**, 20012–20017 (2012).
105. Sharonov, A. & Hochstrasser, R. M. Wide-field subdiffraction imaging by accumulated binding of diffusing probes. *Proc. Natl Acad. Sci. USA* **103**, 18911–18916 (2006).
106. Jungmann, R. et al. Single-molecule kinetics and super-resolution microscopy by fluorescence imaging of transient binding on DNA origami. *Nano Lett.* **10**, 4756–4761 (2010).
107. Schnitzbauer, J., Strauss, M. T., Schlichthaerle, T., Schueder, F. & Jungmann, R. Super-resolution microscopy with DNA-PAINT. *Nat. Protoc.* **12**, 1198–1228 (2017).
108. Lund, K. et al. Molecular robots guided by prescriptive landscapes. *Nature* **465**, 206–210 (2010).
109. Zhao, Z. et al. Nanocaged enzymes with enhanced catalytic activity and increased stability against protease digestion. *Nat. Commun.* **7**, 10619 (2016).
110. Kopperger, E. et al. A self-assembled nanoscale robotic arm controlled by electric fields. *Science* **359**, 296–301 (2018).
111. Thomsen, R. P. et al. A large size-selective DNA nanopore with sensing applications. *Nat. Commun.* **10**, 5655 (2019).
112. Shrestha, P. et al. Mechanical properties of DNA origami nanoassemblies are determined by Holliday junction mechanophores. *Nucleic Acids Res.* **44**, 6574–6582 (2016).
113. Engel, M. C. et al. Force-induced unravelling of DNA origami. *ACS Nano* **12**, 6734–6747 (2018).
114. Shrestha, P. et al. Confined space facilitates G-quadruplex formation. *Nat. Nanotechnol.* **12**, 582–588 (2017).
115. Iwaki, M., Wickham, S. F., Ikezaki, K., Yanagida, T. & Shih, W. M. A programmable DNA origami nanospring that reveals force-induced adjacent binding of myosin VI heads. *Nat. Commun.* **7**, 13715 (2016).
116. Madsen, M. & Gothelf, K. V. Chemistries for DNA nanotechnology. *Chem. Rev.* **119**, 6384–6458 (2019).
117. Tian, Y. et al. Prescribed nanoparticle cluster architectures and low-dimensional arrays built using octahedral DNA origami frames. *Nat. Nanotechnol.* **10**, 637–644 (2015).
118. Kuzyk, A. et al. DNA-based self-assembly of chiral plasmonic nanostructures with tailored optical response. *Nature* **483**, 311–314 (2012).
119. Hartl, C. et al. Position accuracy of gold nanoparticles on DNA origami structures studied with small-angle X-ray scattering. *Nano Lett.* **18**, 2609–2615 (2018).
120. Kuzyk, A. et al. Reconfigurable 3D plasmonic metamolecules. *Nat. Mater.* **13**, 862–866 (2014).
121. Pal, S. et al. DNA directed self-assembly of anisotropic plasmonic nanostructures. *J. Am. Chem. Soc.* **133**, 17606–17609 (2011).
122. Zhang, Y. et al. Nanoparticle-assisted alignment of carbon nanotubes on DNA origami. *Angew. Chem. Int. Ed.* **59**, 4892–4896 (2020).
123. Pei, H. et al. Organizing end-site-specific SWCNTs in specific loci using DNA. *J. Am. Chem. Soc.* **141**, 11923–11928 (2019).
124. Liu, W. Y., Halverson, J., Tian, Y., Tkachenko, A. V. & Gang, O. Self-organized architectures from assorted DNA-framed nanoparticles. *Nat. Chem.* **8**, 867–873 (2016).
125. Liu, W. et al. Diamond family of nanoparticle superlattices. *Science* **351**, 582–586 (2016).
This study creates a diamond superlattice via the constrained packing of triangular binding footprints of DNA origami tetrahedra.
126. Tian, Y. et al. Lattice engineering through nanoparticle–DNA frameworks. *Nat. Mater.* **15**, 654–661 (2016).
127. Zhan, P. et al. Reconfigurable three-dimensional gold nanorod plasmonic nanostructures organized on DNA origami tripod. *ACS Nano* **11**, 1172–1179 (2017).
128. Liu, J. F. et al. Metallization of branched DNA origami for nanoelectronic circuit fabrication. *ACS Nano* **5**, 2240–2247 (2011).
129. Pilo-Pais, M., Goldberg, S., Samano, E., Labean, T. H. & Finkelstein, G. Connecting the nanodots: programmable nanofabrication of fused metal shapes on DNA templates. *Nano Lett.* **11**, 3489–3492 (2011).
130. Schreiber, R. et al. DNA origami-templated growth of arbitrarily shaped metal nanoparticles. *Small* **7**, 1795–1799 (2011).
131. Jia, S. et al. Programming DNA origami patterning with non-canonical DNA-based metallization reactions. *Nat. Commun.* **10**, 5597 (2019).
132. Shang, Y. et al. Site-specific synthesis of silica nanostructures on DNA origami templates. *Adv. Mater.* **32**, 2000294 (2020).
133. Bayrak, T. et al. DNA-mold templated assembly of conductive gold nanowires. *Nano Lett.* **18**, 2116–2123 (2018).
134. Nguyen, L., Doblinger, M., Liedl, T. & Heuer-Jungemann, A. DNA origami-templated silica growth by sol-gel chemistry. *Angew. Chem. Int. Ed.* **58**, 912–916 (2019).
135. Zhang, Y. et al. Transfer of two-dimensional oligonucleotide patterns onto stereocontrolled plasmonic nanostructures through DNA origami-based nanoimprinting lithography. *Angew. Chem. Int. Ed.* **55**, 8036–8040 (2016).
136. Gallego, I. et al. DNA origami-driven lithography for patterning on gold surfaces with sub-10 nm resolution. *Adv. Mater.* **29**, 1603233 (2017).
137. Tian, C. et al. DNA nanostructures-mediated molecular imprinting lithography. *ACS Nano* **11**, 227–238 (2017).
138. Hung, A. M. et al. Large-area spatially ordered arrays of gold nanoparticles directed by lithographically confined DNA origami. *Nat. Nanotechnol.* **5**, 121–126 (2010).
139. Gopinath, A., Miyazono, E., Faraon, A. & Rothemund, P. W. Engineering and mapping nanocavity emission via precision placement of DNA origami. *Nature* **535**, 401–405 (2016).
140. Kershner, R. J. et al. Placement and orientation of individual DNA shapes on lithographically patterned surfaces. *Nat. Nanotechnol.* **4**, 557–561 (2009).
141. Hentschel, M., Schäferling, M., Duan, X., Giessen, H. & Liu, N. Chiral plasmonics. *Sci. Adv.* **3**, e1602735 (2017).
142. Fang, W. et al. Quantizing single-molecule surface-enhanced Raman scattering with DNA origami metamolecules. *Sci. Adv.* **5**, eaau4506 (2019).
143. Weller, L. et al. Gap-dependent coupling of Ag–Au nanoparticle heterodimers using DNA origami-based self-assembly. *ACS Photonics* **3**, 1589–1595 (2016).
144. Roller, E. M. et al. Hotspot-mediated non-dissipative and ultrafast plasmon passage. *Nat. Phys.* **13**, 761–765 (2017).
145. Vogele, K. et al. Self-assembled active plasmonic waveguide with a peptide-based thermomechanical switch. *ACS Nano* **10**, 11377–11384 (2016).
146. Shen, X. et al. Rolling up gold nanoparticle-dressed DNA origami into three-dimensional plasmonic chiral nanostructures. *J. Am. Chem. Soc.* **134**, 146–149 (2012).
147. Urban, M. J. et al. Plasmonic toroidal metamolecules assembled by DNA origami. *J. Am. Chem. Soc.* **138**, 5495–5498 (2016).
148. Shen, X. B. et al. Three-dimensional plasmonic chiral tetramers assembled by DNA origami. *Nano Lett.* **13**, 2128–2133 (2013).
149. Lan, X. et al. Bifacial DNA origami-directed discrete, three-dimensional, anisotropic plasmonic nanoarchitectures with tailored optical chirality. *J. Am. Chem. Soc.* **135**, 11441–11444 (2013).
150. Lan, X. et al. Au nanorod helical superstructures with designed chirality. *J. Am. Chem. Soc.* **137**, 457–462 (2015).
151. Zhou, C., Duan, X. Y. & Liu, N. A plasmonic nanorod that walks on DNA origami. *Nat. Commun.* **6**, 8102 (2015).
152. Urban, M. J. et al. Gold nanocrystal-mediated sliding of doublet DNA origami filaments. *Nat. Commun.* **9**, 1454 (2018).
153. Zhou, X. et al. Efficient long-range, directional energy transfer through DNA-templated dye aggregates. *J. Am. Chem. Soc.* **141**, 8473–8481 (2019).
154. Samanta, A., Zhou, Y., Zou, S., Yan, H. & Liu, Y. Fluorescence quenching of quantum dots by gold nanoparticles: a potential long range spectroscopic ruler. *Nano Lett.* **14**, 5052–5057 (2014).
155. Thacker, V. V. et al. DNA origami based assembly of gold nanoparticle dimers for surface-enhanced Raman scattering. *Nat. Commun.* **5**, 3448 (2014).
156. Acuna, G. P. et al. Fluorescence enhancement at docking sites of DNA-directed self-assembled nanoantennas. *Science* **338**, 506–510 (2012).
157. Puchkova, A. et al. DNA origami nanoantennas with over 5000-fold fluorescence enhancement and single-molecule detection at 25 μM. *Nano Lett.* **15**, 8354–8359 (2015).
158. Zhao, M. et al. DNA-directed nanofabrication of high-performance carbon nanotube field-effect transistors. *Science* **368**, 878–881 (2020).
159. Fu, J. L. et al. DNA-scaffolded proximity assembly and confinement of multienzyme reactions. *Top. Curr. Chem.* **378**, 38 (2020).
160. Niemeyer, C. M., Koehler, J. & Wuerdemann, C. DNA-directed assembly of bienzymic complexes from in vivo biotinylated NAD(P)H:FMN oxidoreductase and luciferase. *ChemBioChem* **3**, 242–245 (2002).
161. Wilner, O. I. et al. Enzyme cascades activated on topologically programmed DNA scaffolds. *Nat. Nanotechnol.* **4**, 249–254 (2009).
162. Fu, J., Liu, M., Liu, Y., Woodbury, N. W. & Yan, H. Interenzyme substrate diffusion for an enzyme cascade organized on spatially addressable DNA nanostructures. *J. Am. Chem. Soc.* **134**, 5516–5519 (2012).
163. Liu, M. et al. A three-enzyme pathway with an optimised geometric arrangement to facilitate substrate transfer. *ChemBioChem* **17**, 1097–1101 (2016).
164. Fu, J. et al. Assembly of multienzyme complexes on DNA nanostructures. *Nat. Protoc.* **11**, 2243–2273 (2016).
165. Zhang, Y., Tsitkov, S. & Hess, H. Proximity does not contribute to activity enhancement in the glucose oxidase–horseradish peroxidase cascade. *Nat. Commun.* **7**, 13982 (2016).
166. Kuzmak, A., Carmali, S., von Lieres, E., Russell, A. J. & Kondrat, S. Can enzyme proximity accelerate cascade reactions? *Sci. Rep.* **9**, 455 (2019).

167. Sprengel, A. et al. Tailored protein encapsulation into a DNA host using geometrically organized supramolecular interactions. *Nat. Commun.* **8**, 14472 (2017).
168. Kohman, R. E., Cha, S. S., Man, H. Y. & Han, X. Light-triggered release of bioactive molecules from DNA nanostructures. *Nano Lett.* **16**, 2781–2785 (2016).
169. Fu, Y. et al. Single-step rapid assembly of DNA origami nanostructures for addressable nanoscale bioreactors. *J. Am. Chem. Soc.* **135**, 696–702 (2013).
170. Linko, V., Eerikainen, M. & Kostiainen, M. A. A modular DNA origami-based enzyme cascade nanoreactor. *Chem. Commun.* **51**, 5351–5354 (2015).
171. Zhang, Y. F. & Hess, H. Toward rational design of high-efficiency enzyme cascades. *ACS Catal.* **7**, 6018–6027 (2017).
172. Adleman, L. M. Molecular computation of solutions to combinatorial problems. *Science* **266**, 1021–1024 (1994).
173. Phillips, A. & Cardelli, L. A programming language for composable DNA circuits. *J. R. Soc. Interface* **6**, S419–436 (2009).
174. Qian, L. & Winfree, E. Scaling up digital circuit computation with DNA strand displacement cascades. *Science* **332**, 1196–1201 (2011).
175. Chatterjee, G., Dalchau, N., Muscat, R. A., Phillips, A. & Seelig, G. A spatially localized architecture for fast and modular DNA computing. *Nat. Nanotechnol.* **12**, 920–927 (2017).
176. Dalchau, N., Chandran, H., Gopalkrishnan, N., Phillips, A. & Reif, J. Probabilistic analysis of localized DNA hybridization circuits. *Acs Synth. Biol.* **4**, 898–913 (2015).
177. Wickham, S. F. J. et al. A DNA-based molecular motor that can navigate a network of tracks. *Nat. Nanotechnol.* **7**, 169–173 (2012).
178. Boemo, M. A., Lucas, A. E., Turberfield, A. J. & Cardelli, L. The formal language and design principles of autonomous DNA walker circuits. *ACS Synth. Biol.* **5**, 878–884 (2016).
179. Gu, H., Chao, J., Xiao, S. J. & Seeman, N. C. A proximity-based programmable DNA nanoscale assembly line. *Nature* **465**, 202–205 (2010). **This study demonstrates a DNA walker that can move on a DNA origami track while collecting proximal cargo molecules on the way, which inspires later studies on DNA machines and robots**.
180. Wang, D. et al. Molecular logic gates on DNA origami nanostructures for microRNA diagnostics. *Anal. Chem.* **86**, 1932–1936 (2014).
181. Amir, Y. et al. Universal computing by DNA origami robots in a living animal. *Nat. Nanotechnol.* **9**, 353–357 (2014).
182. Woods, D. et al. Diverse and robust molecular algorithms using reprogrammable DNA self-assembly. *Nature* **567**, 366–372 (2019).
183. Liu, H., Wang, J., Song, S., Fan, C. & Gothelf, K. V. A DNA-based system for selecting and displaying the combined result of two input variables. *Nat. Commun.* **6**, 10089 (2015).
184. Douglas, S. M., Bachelet, I. & Church, G. M. A logic-gated nanorobot for targeted transport of molecular payloads. *Science* **335**, 831–834 (2012). **This study reports a device controlled by an aptamer-encoded logic gate, enabling it to expose the payloads conditionally in response to different cues on the cell surface**.
185. DeLuca, M., Shi, Z., Castro, C. E. & Arya, G. Dynamic DNA nanotechnology: toward functional nanoscale devices. *Nanoscale Horiz.* **5**, 182–201 (2020).
186. Zhang, Y. et al. Dynamic DNA structures. *Small* **15**, e1900228 (2019).
187. Li, C.-Y. et al. Ionic conductivity, structural deformation, and programmable anisotropy of DNA origami in electric field. *ACS Nano* **9**, 1420–1433 (2015).
188. Kroener, F., Heerwig, A., Kaiser, W., Mertig, M. & Rant, U. Electrical actuation of a DNA origami nanolever on an electrode. *J. Am. Chem. Soc.* **139**, 16510–16513 (2017).
189. Kuzyk, A., Yurke, B., Toppari, J. J., Linko, V. & Törmä, P. Dielectrophoretic trapping of DNA origami. *Small* **4**, 447–450 (2008).
190. Marras, A. E., Zhou, L., Su, H. J. & Castro, C. E. Programmable motion of DNA origami mechanisms. *Proc. Natl Acad. Sci. USA* **112**, 713–718 (2015).
191. Ramezani, H. & Dietz, H. Building machines with DNA molecules. *Nat. Rev. Genet.* **21**, 5–26 (2020).
192. Pezzato, C., Cheng, C., Stoddart, J. F. & Astumian, R. D. Mastering the non-equilibrium assembly and operation of molecular machines. *Chem. Soc. Rev.* **46**, 5491–5507 (2017).
193. Bazrafshan, A. et al. Tunable DNA origami motors translocate ballistically over μm distances at nm/s speeds. *Angew. Chem. Int. Ed.* **59**, 9514–9521 (2020).
194. Zhang, Q. et al. DNA origami as an in vivo drug delivery vehicle for cancer therapy. *ACS Nano* **8**, 6633–6643 (2014).
195. Jiang, D. et al. DNA origami nanostructures can exhibit preferential renal uptake and alleviate acute kidney injury. *Nat. Biomed. Eng.* **2**, 865–877 (2018).
196. Jiang, Q. et al. DNA origami as a carrier for circumvention of drug resistance. *J. Am. Chem. Soc.* **134**, 13396–13403 (2012).
197. Zhao, Y.-X. et al. DNA origami delivery system for cancer therapy with tunable release properties. *ACS Nano* **6**, 8684–8691 (2012).
198. Schüller, V. J. et al. Cellular immunostimulation by CpG-sequence-coated DNA origami structures. *ACS Nano* **5**, 9696–9702 (2011).
199. Liu, S. et al. A DNA nanodevice-based vaccine for cancer immunotherapy. *Nat. Mater.* https://doi.org/10.1038/s41563-020-0793-6 (2020).
200. Rahman, M. A. et al. Systemic delivery of Bc12-targeting siRNA by DNA nanoparticles suppresses cancer cell growth. *Angew. Chem. Int. Ed.* **56**, 16023–16027 (2017).
201. Lee, H. et al. Molecularly self-assembled nucleic acid nanoparticles for targeted in vivo siRNA delivery. *Nat. Nanotechnol.* **7**, 389–393 (2012).
202. Mei, Q. et al. Stability of DNA origami nanoarrays in cell lysate. *Nano Lett.* **11**, 1477–1482 (2011).
203. Li, J. et al. Self-assembled multivalent DNA nanostructures for noninvasive intracellular delivery of immunostimulatory CpG oligonucleotides. *ACS Nano* **5**, 8783–8789 (2011).
204. Liang, L. et al. Single-particle tracking and modulation of cell entry pathways of a tetrahedral DNA nanostructure in live cells. *Angew. Chem. Int. Ed.* **53**, 7745–7750 (2014).
205. Bhatia, D., Surana, S., Chakraborty, S., Koushika, S. P. & Krishnan, Y. A synthetic icosahedral DNA-based host–cargo complex for functional in vivo imaging. *Nat. Commun.* **2**, 339 (2011).
206. Modi, S. et al. A DNA nanomachine that maps spatial and temporal pH changes inside living cells. *Nat. Nanotechnol.* **4**, 325–330 (2009).
207. Zhang, H. et al. DNA nanostructures coordinate gene silencing in mature plants. *Proc. Natl. Acad. Sci. USA* **116**, 7543–7548 (2019).
208. Zhang, H. et al. Engineering DNA nanostructures for siRNA delivery in plants. *Nat. Protoc.* **15**, 3064–3087 (2020).
209. Wang, P. et al. Visualization of the cellular uptake and trafficking of DNA origami nanostructures in cancer cells. *J. Am. Chem. Soc.* **140**, 2478–2484 (2018). **This study presents a visualization of the cellular uptake and trafficking of DNA origami nanostructures in cancer cells**.
210. Bastings, M. M. C. et al. Modulation of the cellular uptake of DNA origami through control over mass and shape. *Nano Lett.* **18**, 3557–3564 (2018).
211. Wiraja, C. et al. Framework nucleic acids as programmable carrier for transdermal drug delivery. *Nat. Commun.* **10**, 1147 (2019).
212. Poon, W., Kingston, B. R., Ouyang, B., Ngo, W. & Chan, W. C. W. A framework for designing delivery systems. *Nat. Nanotechnol.* **15**, 819–829 (2020).
213. Mikkila, J. et al. Virus-encapsulated DNA origami nanostructures for cellular delivery. *Nano Lett.* **14**, 2196–2200 (2014).
214. Schaffert, D. H. et al. Intracellular delivery of a planar DNA origami structure by the transferrin-receptor internalization pathway. *Small* **12**, 2634–2640 (2016).
215. Veneziano, R. et al. Role of nanoscale antigen organization on B-cell activation probed using DNA origami. *Nat. Nanotechnol.* **15**, 716–723 (2020).
216. Surana, S., Shenoy, A. R. & Krishnan, Y. Designing DNA nanodevices for compatibility with the immune system of higher organisms. *Nat. Nanotechnol.* **10**, 741–747 (2015). **This perspective article discusses the immunocompatibility issues of DNA nanotechnology in biomedical applications and proposes possible strategies that could either evade or stimulate the host response**.
217. Engelhardt, F. A. S. et al. Custom-size, functional, and durable DNA origami with design-specific scaffolds. *ACS Nano* **13**, 5015–5027 (2019).
218. Auvinen, H. et al. Protein coating of DNA nanostructures for enhanced stability and immunocompatibility. *Adv. Healthc. Mater.* **6**, 1700692 (2017).
219. Steinhauer, C., Jungmann, R., Sobey, T. L., Simmel, F. C. & Tinnefeld, P. DNA origami as a nanoscopic ruler for super-resolution microscopy. *Angew. Chem. Int. Ed.* **48**, 8870–8873 (2009).
220. Schmied, J. J. et al. DNA origami-based standards for quantitative fluorescence microscopy. *Nat. Protoc.* **9**, 1367–1391 (2014).
221. Zanacchi, F. C. et al. A DNA origami platform for quantifying protein copy number in super-resolution. *Nat. Methods* **14**, 789–792 (2017).
222. Jungmann, R. et al. Quantitative super-resolution imaging with qPAINT. *Nat. Methods* **13**, 439–442 (2016).
223. Kosuri, P., Altheimer, B. D., Dai, M., Yin, P. & Zhuang, X. Rotation tracking of genome-processing enzymes using DNA origami rotors. *Nature* **572**, 136–140 (2019).
224. Pfitzner, E. et al. Rigid DNA beams for high-resolution single-molecule mechanics. *Angew. Chem. Int. Ed.* **52**, 7766–7771 (2013).
225. Kilchherr, F. et al. Single-molecule dissection of stacking forces in DNA. *Science* **353**, aaf5508 (2016).
226. Dutta, P. K. et al. Programmable multivalent DNA origami tension probes for reporting cellular traction forces. *Nano Lett.* **18**, 4803–4811 (2018).
227. Hariadi, R. F. et al. Mechanical coordination in motor ensembles revealed using engineered artificial myosin filaments. *Nat. Nanotechnol.* **10**, 696–700 (2015).
228. Iwaki, M., Iwane, A. H., Ikezaki, K. & Yanagida, T. Local heat activation of single myosins based on optical trapping of gold nanoparticles. *Nano Lett.* **15**, 2456–2461 (2015).
229. Derr, N. D. et al. Tug-of-war in motor protein ensembles revealed with a programmable DNA origami scaffold. *Science* **338**, 662–665 (2012).
230. Endo, M. & Sugiyama, H. Single-molecule imaging of dynamic motions of biomolecules in DNA origami nanostructures using high-speed atomic force microscopy. *Acc. Chem. Res.* **47**, 1645–1653 (2014).
231. Rajendran, A., Endo, M., Hidaka, K. & Sugiyama, H. Direct and real-time observation of rotary movement of a DNA nanomechanical device. *J. Am. Chem. Soc.* **135**, 1117–1123 (2013).
232. Endo, M. et al. Direct visualization of the movement of a single T7RNA polymerase and transcription on a DNA nanostructure. *Angew. Chem. Int. Ed.* **51**, 8778–8782 (2012).
233. Suzuki, Y. et al. DNA origami based visualization system for studying site-specific recombination events. *J. Am. Chem. Soc.* **136**, 211–218 (2014).
234. Endo, M., Katsuda, Y., Hidaka, K. & Sugiyama, H. Regulation of DNA methylation using different tensions of double strands constructed in a defined DNA nanostructure. *J. Am. Chem. Soc.* **132**, 1592–1597 (2010).
235. Wickham, S. F. J. et al. Direct observation of stepwise movement of a synthetic molecular transporter. *Nat. Nanotechnol.* **6**, 166–169 (2011).
236. Funke, J. J. & Dietz, H. Placing molecules with Bohr radius resolution using DNA origami. *Nat. Nanotechnol.* **11**, 47–52 (2016).
237. Funke, J. J., Ketterer, P., Lieleg, C., Korber, P. & Dietz, H. Exploring nucleosome unwrapping using DNA origami. *Nano Lett.* **16**, 7891–7898 (2016).
238. Funke, J. J. et al. Uncovering the forces between nucleosomes using DNA origami. *Sci. Adv.* **2**, e1600974 (2016).
239. Le, J. V. et al. Probing nucleosome stability with a DNA origami nanocaliper. *ACS Nano* **10**, 7073–7084 (2016).
240. Nickels, P. C. et al. Molecular force spectroscopy with a DNA origami-based nanoscopic force clamp. *Science* **354**, 305–307 (2016).
241. Xiong, Q. et al. DNA origami post-processing by CRISPR–Cas12a. *Angew. Chem. Int. Ed.* **59**, 3956–3960 (2020).
242. Kramm, K. et al. DNA origami-based single-molecule force spectroscopy elucidates RNA polymerase III pre-initiation complex stability. *Nat. Commun.* **11**, 2828 (2020).
243. Martin, T. G. et al. Design of a molecular support for cryo-EM structure determination. *Proc. Natl Acad. Sci. USA* **113**, E7456–E7463 (2016).
244. Dong, Y. et al. Folding DNA into a lipid-conjugated nanobarrel for controlled reconstitution of membrane proteins. *Angew. Chem. Int. Ed.* **57**, 2072–2076 (2018).
245. Aksel, T., Yu, Z., Cheng, Y. & Douglas, S. M. Molecular goniometers for single-particle cryo-electron microscopy of DNA-binding proteins. *Nat. Biotechnol.* https://doi.org/10.1038/s41587-020-0716-8 (2020).

246. Rinker, S. et al. Self-assembled DNA anostructures for distance-dependent multivalent ligand–protein binding. *Nat. Nanotechnol.* **3**, 418–422 (2008).
247. Shaw, A. et al. Binding to nanopatterned antigens is dominated by the spatial tolerance of antibodies. *Nat. Nanotechnol.* **14**, 184–190 (2019).
248. Zhang, P. et al. Capturing transient antibody conformations with DNA origami epitopes. *Nat. Commun.* **11**, 3114 (2020).
249. Wang, F. et al. Programming PAM antennae for efficient CRISPR–Cas9 DNA editing. *Sci. Adv.* **6**, eaay9948 (2020).
250. Fisher, P. D. E. et al. A programmable DNA origami platform for organizing intrinsically disordered nucleoporins within nanopore confinement. *ACS Nano* **12**, 1508–1518 (2018).
251. Ketterer, P. et al. DNA origami scaffold for studying intrinsically disordered proteins of the nuclear pore complex. *Nat. Commun.* **9**, 902 (2018).
252. Xu, W. et al. A programmable DNA origami platform to organize SNAREs for membrane fusion. *J. Am. Chem. Soc.* **138**, 4439–4447 (2016).
253. Yang, Y. et al. Self-assembly of size-controlled liposomes on DNA nanotemplates. *Nat. Chem.* **8**, 476–483 (2016).
254. Zhang, Z., Yang, Y., Pincet, F., Llaguno, M. C. & Lin, C. Placing and shaping liposomes with reconfigurable DNA nanocages. *Nat. Chem.* **9**, 653–659 (2017).
255. Bian, X., Zhang, Z., Xiong, Q., De Camilli, P. & Lin, C. A programmable DNA origami platform for studying lipid transfer between bilayers. *Nat. Chem. Biol.* **15**, 830–837 (2019).
256. Czogalla, A. et al. Amphipathic DNA origami nanoparticles to scaffold and deform lipid membrane vesicles. *Angew. Chem. Int. Ed.* **54**, 6501–6505 (2015).
257. Franquelim, H. G., Khmelinskaia, A., Sobczak, J.-P., Dietz, H. & Schwille, P. Membrane sculpting by curved DNA origami scaffolds. *Nat. Commun.* **9**, 811 (2018).
258. Grome, M. W., Zhang, Z., Pincet, F. & Lin, C. Vesicle tubulation with self-assembling DNA nanosprings. *Angew. Chem. Int. Ed.* **57**, 5330–5334 (2018).
259. Grome, M. W., Zhang, Z. & Lin, C. Stiffness and membrane anchor density modulate DNA-nanospring-induced vesicle tubulation. *ACS Appl. Mater. Interfaces* **11**, 22987–22992 (2019).
260. Journot, C. M. A., Ramakrishna, V., Wallace, M. I. & Turberfield, A. J. Modifying membrane morphology and interactions with DNA origami clathrin-mimic networks. *ACS Nano* **13**, 9973–9979 (2019).
261. Ghenuche, P., de Torres, J., Moparthi, S. B., Grigoriev, V. & Wenger, J. Nanophotonic enhancement of the Forster resonance energy-transfer rate with single nanoapertures. *Nano Lett.* **14**, 4707–4714 (2014).
262. Engst, C. R. et al. DNA origami nanopores. *Nano Lett.* **12**, 512–517 (2012).
263. Wei, R., Martin, T. G., Rant, U. & Dietz, H. DNA origami gatekeepers for solid-state nanopores. *Angew. Chem. Int. Ed.* **51**, 4864–4867 (2012).
264. Saccà, B. & Niemeyer, C. M. DNA origami: the art of folding DNA. *Angew. Chem. Int. Ed.* **51**, 58–66 (2012).
265. Xin, Y. et al. Cryopreservation of DNA origami nanostructures. *Small* **16**, 1905959 (2020).
266. Ponnuswamy, N. et al. Oligolysine-based coating protects DNA nanostructures from low-salt denaturation and nuclease degradation. *Nat. Commun.* **8**, 15654 (2017).
267. Birac, J. J., Sherman, W. B., Kopatsch, J., Constantinou, P. E. & Seeman, N. C. Architecture with GIDEON, a program for design in structural DNA nanotechnology. *J. Mol. Graph. Model.* **25**, 470–480 (2006).
268. Ke, Y. et al. Multilayer DNA origami packed on a square lattice. *J. Am. Chem. Soc.* **131**, 15903–15908 (2009).
269. Williams, S. et al. in *DNA Computing* Vol. 5347 (eds Goel, A., Simmel, F. C. & Sosik, P.) 90–101 (Springer, 2009).
270. Kim, D.-N., Kilchherr, F., Dietz, H. & Bathe, M. Quantitative prediction of 3D solution shape and flexibility of nucleic acid nanostructures. *Nucleic Acids Res.* **40**, 2862–2868 (2011).
271. Ouldridge, T. E., Louis, A. A. & Doye, J. P. K. Structural, mechanical, and thermodynamic properties of a coarse-grained DNA model. *J. Chem. Phys.* **134**, 085101 (2011).
272. Sharma, R., Schreck, J. S., Romano, F., Louis, A. A. & Doye, J. P. K. Characterizing the motion of jointed DNA nanostructures using a coarse-grained model. *ACS Nano* **11**, 12426–12435 (2017).
273. Shi, Z., Castro, C. E. & Arya, G. Conformational dynamics of mechanically compliant DNA nanostructures from coarse-grained molecular dynamics simulations. *ACS Nano* **11**, 4617–4630 (2017).
274. Huang, C.-M., Kucinic, A., Le, J. V., Castro, C. E. & Su, H.-J. Uncertainty quantification of a DNA origami mechanism using a coarse-grained model and kinematic variance analysis. *Nanoscale* **11**, 1647–1660 (2019).
275. Stephanopoulos, N. Peptide–oligonucleotide hybrid molecules for bioactive nanomaterials. *Bioconjugate Chem.* **30**, 1915–1922 (2019).
276. Yang, Y. R., Liu, Y. & Yan, H. DNA nanostructures as programmable biomolecular scaffolds. *Bioconjugate Chem.* **26**, 1381–1395 (2015).
This review focuses on using DNA nanostructures to precisely programme the spatial arrangements of biomolecules, especially proteins, which is fundamental in applications including catalysis, drug delivery, bioimaging and biophysics.
277. Marras, A. E., Zhou, L., Kolliopoulos, V., Su, H. J. & Castro, C. E. Directing folding pathways for multi-component DNA origami nanostructures with complex topology. *N. J. Phys.* **18**, 055005 (2016).
278. Myhrvold, C. et al. Barcode extension for analysis and reconstruction of structures. *Nat. Commun.* **8**, 14698 (2017).
279. Iinuma, R. et al. Polyhedra self-assembled from DNA tripods and characterized with 3D DNA-PAINT. *Science* **344**, 65–69 (2014).
280. Zhao, Z., Yan, H. & Liu, Y. A route to scale up DNA origami using DNA tiles as folding staples. *Angew. Chem. Int. Ed.* **49**, 1414–1417 (2010).
281. Zhao, Z., Liu, Y. & Yan, H. Organizing DNA origami tiles into larger structures using preformed scaffold frames. *Nano Lett.* **11**, 2997–3002 (2011).
282. Woo, S. & Rothemund, P. W. K. Self-assembly of two-dimensional DNA origami lattices using cation-controlled surface diffusion. *Nat. Commun.* **5**, 4889 (2014).
283. Ducani, C., Kaul, C., Moche, M., Shih, W. M. & Högberg, B. Enzymatic production of 'monoclonal stoichiometric' single-stranded DNA oligonucleotides. *Nat. Methods* **10**, 647–652 (2013).
284. Schmidt, T. L. et al. Scalable amplification of strand subsets from chip-synthesized oligonucleotide libraries. *Nat. Commun.* **6**, 8634 (2015).
285. Praetorius, F. et al. Biotechnological mass production of DNA origami. *Nature* **552**, 84–87 (2017).
286. Gerling, T., Kube, M., Kick, B. & Dietz, H. Sequence-programmable covalent bonding of designed DNA assemblies. *Sci. Adv.* **4**, eaau1157 (2018).
287. Cassinelli, V. et al. One-step formation of "chain-armor"-stabilized DNA nanostructures. *Angew. Chem. Int. Ed.* **54**, 7795–7798 (2015).
288. Chopra, A., Krishnan, S. & Simmel, F. C. Electrotransfection of polyamine folded DNA origami structures. *Nano Lett.* **16**, 6683–6690 (2016).
289. Ahmadi, Y., De Llano, E. & Barišić, I. (Poly)Cation-induced protection of conventional and wireframe DNA origami nanostructures. *Nanoscale* **10**, 7494–7504 (2018).
290. Wang, S.-T. et al. DNA origami protection and molecular interfacing through engineered sequence-defined peptoids. *Proc. Natl Acad. Sci. USA* **117**, 6339–6348 (2020).
291. Perkel, J. M. The race for enzymatic DNA synthesis heats up. *Nature* **566**, 565 (2019).
292. He, Y. & Liu, D. R. Autonomous multistep organic synthesis in a single isothermal solution mediated by a DNA walker. *Nat. Nanotechnol.* **5**, 778–782 (2010).
293. Meng, W. et al. An autonomous molecular assembler for programmable chemical synthesis. *Nat. Chem.* **8**, 542–548 (2016).
294. Lauback, S. et al. Real-time magnetic actuation of DNA nanodevices via modular integration with stiff micro-levers. *Nat. Commun.* **9**, 1446 (2018).
295. Murugan, A., Zeravcic, Z., Brenner, M. P. & Leibler, S. Multifarious assembly mixtures: systems allowing retrieval of diverse stored structures. *Proc. Natl Acad. Sci. USA* **112**, 54–59 (2015).
296. He, X. et al. Exponential growth and selection in self-replicating materials from DNA origami rafts. *Nat. Mater.* **16**, 993–997 (2017).
297. Pinheiro, V. B. et al. Synthetic genetic polymers capable of heredity and evolution. *Science* **336**, 341–344 (2012).
298. Hoshika, S. et al. Hachimoji DNA and RNA: a genetic system with eight building blocks. *Science* **363**, 884–887 (2019).
299. Geary, C., Rothemund, P. W. & Andersen, E. S. RNA nanostructures. A single-stranded architecture for cotranscriptional folding of RNA nanostructures. *Science* **345**, 799–804 (2014).
300. Zhang, Y. et al. A semi-synthetic organism that stores and retrieves increased genetic information. *Nature* **551**, 644–647 (2017).
301. Matthies, M. et al. Triangulated wireframe structures assembled using single-stranded DNA tiles. *ACS Nano* **13**, 1839–1848 (2019).
302. Dai, M., Jungmann, R. & Yin, P. Optical imaging of individual biomolecules in densely packed clusters. *Nat. Nanotechnol.* **11**, 798–807 (2016).
303. Praetorius, F. & Dietz, H. Self-assembly of genetically encoded DNA–protein hybrid nanoscale shapes. *Science* **355**, eaam5488 (2017).
304. Li, M. et al. In vivo production of RNA nanostructures via programmed folding of single-stranded RNAs. *Nat. Commun.* **9**, 2196 (2018).
305. Voigt, N. V. et al. Single-molecule chemical reactions on DNA origami. *Nat. Nanotechnol.* **5**, 200–203 (2010).
306. Langecker, M. et al. Synthetic lipid membrane channels formed by designed DNA nanostructures. *Science* **338**, 932–936 (2012).
307. Knudsen, J. B. et al. Routing of individual polymers in designed patterns. *Nat. Nanotechnol.* **10**, 892–898 (2015).
308. Li, N. et al. Precise organization of metal and metal oxide nanoclusters into arbitrary patterns on DNA origami. *J. Am. Chem. Soc.* **141**, 17968–17972 (2019).
309. Aghebat Rafat, A., Sagredo, S., Thalhammer, M. & Simmel, F. C. Barcoded DNA origami structures for multiplexed optimization and enrichment of DNA-based protein-binding cavities. *Nat. Chem.* **12**, 852–859 (2020).
310. Rosier, B. J. H. M. et al. Proximity-induced caspase-9 activation on a DNA origami-based synthetic apoptosome. *Nat. Catal.* **3**, 295–306 (2020).

Acknowledgements

C.F. and J.L. were supported by the National Natural Science Foundation of China (21991134, 21834007) and the Shanghai Municipal Science and Technology Commission (19JC1410300). K.V.G. and M.A.D.N. were supported by DNA-Based Modular Nanorobotics (DNA-Robotics) and the Marie Curie Innovative Training Network (MRC ITN) under EU H2020 (Project ID: 765703). P.Z. and N.L. were supported by a European Research Council (ERC *Dynamic Nano*) grant. B.S. was supported by the Deutsche Forschungsgemeinschaft (CRC-1093).

Author contributions

Introduction (C.F. and J.L.); Experimentation (S.D., N.L., H.Y. and P.Z.); Results (B.S.); Applications (C.F., J.L., C.L., L.L., K.V.G. and M.A.D.N.); Reproducibility and data deposition (C.F., N.L. and P.Z.); Limitations and optimizations (C.L. and L.L.); Outlook (F.C.S.); Overview of the Primer (C.F.).

Competing interests

C.F. declares an issued Chinese patent (patent number 2018112787266) and a Chinese patent application (2016111794282) based on technologies described in this Primer. F.C.S. has patent applications on DNA origami membrane channels (EP2695949B1) and the electrically driven DNA robotic arm (EP3607646A1). All other authors declare no competing interests.

Peer review information

Nature Reviews Methods Primers thanks A. R. Chandrasekaran, S. Lee, S. Pecic, R. Shetty and the other, anonymous, reviewer(s) for their contribution to the peer review of this work.

Publisher's note

Springer Nature remains neutral with regard to jurisdictional claims in published maps and institutional affiliations.

RELATED LINKS

Adenita: https://www.samson-connect.net/element/dda2a078-1ab6-96ba-0d14-ee1717632d7a.html
CaDNAno: https://cadnano.org/
CanDo: http://cando-DNA-origami.org/
COSM: http://vsb.fbb.msu.ru/cosm
DAEDALUS: http://daedalus-DNA-origami.org/
EMAN2: https://blake.bcm.edu/emanwiki/EMAN2
GenBank: https://www.ncbi.nlm.nih.gov/genbank
METIS: http://metis-DNA-origami.org/
Molecular programming: http://molecular-programming.org/
oxDNA: https://oxdna.org/
oxView: https://sulcgroup.github.io/oxdna-viewer/
PERDIX: http://perdix-DNA-origami.org/
TALOS: http://talos-DNA-origami.org/
Tiamat: http://yanlab.asu.edu/Resources.html
vHelix: http://vhelix.net/